Study on Production of the ω−1 Hydroxy Fatty Acids in the Cyanobacterial Cells

January 2021

Inada Takashi

Study on Production of the ω−1 Hydroxy Fatty Acids in the Cyanobacterial Cells

A dissertation submitted to

the Graduate School of Life and Environmental Science,

the University of Tsukuba

in Partial Fulfillment of the Requirements

for the Degree of Doctor of Philosophy

(Doctoral Program in Integrative Environment and Biomass Sciences)

Inada Takashi

Table of Contents

List of Tables

List of Figures

Abstract

For sustainable development, microalgal lipids and fatty acids (FAs) are very attractive components for biofuel because of the potential high productivity of them. It is also significant to develop microalgal oil as a chemical feedstock for sustainable economic valuable product. In many study, chemical and biological conversion of microalgal oil were investigated in order to adapt to oleochemical industry. FAs which have a hydroxy group adjacent to the end of acyl-chain have potential to utilize as lubricant, cosmetics, anti-biotics, polymer-building block, and anti-cancer agent. Although the hydroxy fatty acids might be an important chemical feedstock, most of the algae do not accumulate it. In this study, I succeed in photoautotrophic production of ω-1 hydroxy fatty acids (ω1HFAs) in cyanobacterium, *Synechocystis* sp. PCC6803 (*Synechocystis*).

To produce hydroxy FAs in *Synechocystis*, 3-hydroxybutylyl-CoA (3HB-CoA), which is an intermediate for polyhydroxybutylate (PHB) biosynthesis in the strain, was utilized as precursor of ω1HFAs. To introduce 3HB-CoA into fatty acid synthesis pathway, I replaced a gene for promiscuous 3-ketoacyl-ACP synthase III from *Alicyclobacillus acidocalderius* (aaKASIII) with the *fabH* gene for native KASIII in *Synechocysitis* (*aaKASIII*+). This *aaKASIII*+ strain did not accumulate ω1HFAs. To increase 3HB-CoA pool for the aaKASIII, the *phaC* gene for PHB polymerase was deleted (*aaKASIII*+/*phaC*-) but ω1HFAs were not observed in the *aaKASIII*+/*phaC*- strain. I also attempted the overexpression of native *phaAB* genes for 3HB-CoA synthesis (*aaKASIII*+/*phaC*-/*SphaAB*+) to enhance 3HB-CoA pool. No ω1HFAs were produced by *aaKASIII*+/*phaC*-/*SphaAB*+. Cultivation under phosphate limited condition with 4% acetate enhance PHB production in *Synechocysitis*. Applying this condition to these three strains which are *aaKASIII*+, *aaKASIII*+/*phaC*-, and *aaKASIII*+/*phaC*-/*SphaAB*+ showed

no effect on production of ω1HFAs. To further enhance 3HB-CoA pool, phaAB from *Cupriavidus necator* H16 which is the high PHB producer were overexpressed (*aaKASIII+*/*phaC-*/*CphaAB+*). The *aaKASIII+*/*phaC-*/*CphaAB+* strain synthesized three types of ω1HFA, 15-hydroxyhexadecanoic acid, 17-hydroxyoctadecanoic acid, and 17-hydroxyoctadec-9-enoic acid. This strain accumulated about 2.1 mol% of the ω1HFA in total FAs under illumination with 70 μmol photons m^{-2} s^{-1}, although the growth of the strain was severely retarded. Under the weak light (35 μmol photons m^{-2} s^{-1}) conditions, this strain grew as well as the wild-type cells and accumulated a much lower amount of the hydroxy FAs, i.e., 0.04 mol%.

To investigate details of the relationship between ω1HFA production and photosynthesis in the *aaKASIII+*/*phaC-*/*CphaAB+* cells, I measured simultaneously ω1HFA contents and photosynthesis-related factors in the cells cultured under the various light conditions, *i.e.*, 35, 70, or 140 μmol photons m^{-2} s^{-1}. The production of the ω1HFA was responded to increasing in the light intensity of cultivation. After the ω1HFA accumulation of the *aaKASIII+*/*phaC-*/*CphaAB+* cells incubated under the illumination of 140 μmol photons m^{-2} s^{-1} at 8 hours, the photosynthesis-related factors such as the chlorophyll content and quantum yield, Fv/Fm, were continuously decreased. These results indicated that the ω1HFA accumulation promoted the photoinhibition.

Lipid separation by TLC showed that the ω1HFAs were not predominantly esterified in galactolipids which are the major lipid classes in cyanobacteria. TLC analysis of lipids from *aaKASIII+*/*phaC-*/*CphaAB+* showed an additional spot migrated under monogalactosyldiacylglycerol (lipid X). The chromatogram of lipid X by liquid chromatography/Mass spectrometry showed five peaks of lipids. The fragmentation pattern indicated that each lipid has hexose as a head group, and the FA pairs of lipids

were estimated as 16:0 OH/18:3, 16:0 OH/18:2, 16:0 OH/18:1, 16:0/18:1 OH, 16:0 OH/18:0 OH. This is the first attempt to produce FAs possessing a functional group near the end of the acyl chain in the photosynthetic organisms.

Keywords: 3-Ketoacyl-ACP Synthase III, Fatty acid synthesis, Bio-based chemicals, Omega-functionalized fatty acids, Metabolic engineering

1. Introduction

Recently, vegetable oils have become an important feedstock for chemicals as they contain lipids and fatty acids (FAs), which are not present in petroleum oil, and large amount of vegetable oils are produced worldwide [1] and used in the oleochemical industry for various applications. To expand the use of lipids and FAs from vegetable oils as raw materials, the synthesis of functionalized FAs by chemical and biotechnological engineering is essential. The hydroxy group is one of the most effective functional groups in the chemical reactivity of FAs, and its positions in the acyl chain play a vital role in its physiological mechanisms and chemical applications [2]. In particular, FAs that have a hydroxy group at the proximity of the ω-position of the acyl chain possess a high availability for various kinds of chemical feedstock, such as adhesives, lubricants, cosmetic intermediates [3], potential anticancer agents [4], and building blocks for the synthesis of polyesters, which exhibit similar or superior physicochemical properties to polyethylene and other bioplastics [5]. FAs with a hydroxy group near the ω-position are naturally produced in a wide variety of organisms [6–8], most of which synthesize these hydroxylated FAs through ω-oxidation by cytochrome P450 monooxygenase. Whole-cell biocatalysis of the enzyme achieves a high conversion ratio of FAs hydroxylation and shows great potential for large-scale production of industrial applications [9].

Microalgal oil is attracting attention as a biofuel because microalgae have the potential to achieve high productivity, cultivate on non-arable land, grow in wastewater, and their cells can be modified by genetic engineering. Despite these advantages, biofuel from microalgae is a controversial technology because several issues remain before achieving economic competitiveness in the production process, i.e., correction of cells, drying of

the cells, and oil extraction. The production of high-value compounds by microalgae is a potential solution to achieve economic competitiveness. As high-value products from microalgal oils, modified fatty acids might be a possible candidate that could be applied for the feedstock of unique compounds. For instance, a wide variety of compounds, such as polyols and polyurethane, are developed from the epoxidation of unsaturated double bonds in FAs from algal lipids [10–12]. For functionalization of the FAs from the microalgal crude oil, FA derivatives, such as dicarboxylic acids and diols, are produced by chemical conversion to add functional groups on the acyl chain of FAs, using a Pd catalyst under CO atmosphere with 20 bar-pressurized conditions [13]. In nature, 3-hydroxy fatty acids previously have been found in the lipopolysaccharides of some cyanobacteria including *Anacystis nidulans* [14], *Anabaena variabilis* [15] and *Synechocystis* strains [16] and some microalgae including *Chlamydomonns reinhardtii*, *Chlorella pyrenoidosa* and *Cyanidium caldarium* [17]. Several microalgae such as *Tetraedron minimum*, *Scenedesmus communis* and *Pediastrum boryanum* produce cell wall-specific ω-hydroxylate C30-34 fatty acids [18,19] which are component of bio-polyester. Recently, the genetically modified diatom *Chaetoceros gracilis,* with the FA dehydrogenase gene from ergot fungus *Claviceps purpurea*, produces ricinoleic acid (12-hydroxy-9-*cis*-octadecanoic acid) [20]. Despite the growth inhibition of yeast or other organisms owing to the production of hydroxy FAs, this diatom can produce ricinoleic acid without growth inhibition because detoxification of hydroxy FA naturally occurs by esterification of the hydroxy group with a carboxyl group on the other FAs. In this diatom, The detoxification mechanism and the effect of hydroxy FA on photosynthesis is unclear [21]. However, there are no studies either to produce FAs that contain a hydroxy group at the proximity of the ω-position by genetic engineering of microalgae, or to investigate

the effect of hydroxy FAs on photosynthesis.

Cyanobacteria are an attractive organism as a microbial factory because they use sunlight and CO_2 as energy and carbon sources to produce biomass via photosynthesis [22–26]. This organism is also utilized as a model to investigate the function and mechanism of photosynthesis. Representative biochemical production by cyanobacteria is poly β-hydroxybutyrate (PHB), which is utilized as a biodegradable polymer, and 3-hydroxybutyrate, which is the precursor of fine chemicals such as antibiotics, pheromones, and amino acids, and cyanobacteria have the intrinsic ability to synthesize PHB and 3-hydroxybutyryl-CoA as a PHB precursor (3) [21,27–30]. To improve PHB productivity on cyanobacteria, optimization of cultivate condition and/or genetic modification were investigated in the previous studies. The nitrogen or phosphate limiting condition with acetate improve PHB production on cyanobacteria [31]. The engineered cyanobacterial strain of overexpression of native PHB synthesis gene cluster also stimulate PHB production, and nutrient limiting condition with acetate further promote PHB accumulation in the strain [32]. For 3-hydroxybutyrate (3HB) production, the introduction of an exogenous gene cluster from a high PHB producer such as *Cupriavidus necator* H16 is more effective than overexpression of native gene cluster for 3HB production on cyanobacteria [33]. A study on the cyanobacteria FAs is significant both in terms of biofuel production and physiological analysis. For biofuel production, overproduction and secretion of free fatty acids are achieved in cyanobacterial strains by genetic manipulations [34–36]. In addition, to obtain cyanobacterial cells that are oxidation-tolerant and maintain the fluidity of membrane lipids, we succeeded in producing FAs such as cyclopropane FAs and 10-methyl stearic acid in transformants of *Synechocystis* sp. PCC 6803 (hereafter *Synechocystis*) [37,38]. These results indicate that

cyanobacteria are a promising organism for application in the modification to produce unnatural FAs. A thorough study on the relationship between FA and photosynthetic pigment in *Synechocystis* can help understand the effects of hydroxy FA production on photosynthesis, which has never been investigated. Regarding biochemical synthesis, cyanobacteria mainly produce glycolipids, i.e., monogalactosyldiacylglycerol (MGDG) and digalactosyldiacylglycerol (DGDG) as the major lipid components, while *Escherichia coli* and *Rhodospirillum rubrum,* which are host organisms for the production of hydroxy FAs in this study, mainly synthesize phospholipids. Glycolipids with hydroxy FAs have the potential to be utilized as novel glycolipid biosurfactants [39].

In this study, we attempted to synthesize ω-1 hydroxy FAs (ω1HFAs) in the cyanobacterium *Synechocystis* by genetic engineering. *Synechocystis* synthesizes 3HB-CoA as a metabolic intermediate in the synthesis of PHB. If 3HB-CoA is incorporated into the *de novo* synthesis pathway of FA instead of acetyl-CoA, it might produce ω1HFAs. To achieve this, the substrate flexibility of β-ketoacyl-ACP-synthase III (KASIII), which is the enzyme for the first reaction of the FA synthesis pathway, is attractive. The reaction by KASIII defines the chemical structure of the ω-end of FAs by the structure of the acyl-CoA moiety and substrate specificity of KASIII. In general, KASIII uses acetyl-CoA as a substrate. *Bacillus subtills* synthesize branched-chain fatty acids from branched-chain acyl-CoA and introduce it instead of acetyl-CoA into fatty acid synthesis pathway by flexible KASIII [40]. Thermo-acidophilic bacilli *Alicyclobacillus* produce ω-alicyclic fatty acids from alicyclic acyl-CoA by flexible KASIII which can introduce sterically bulky acyl-CoA such as cyclohexanecarboxyl-CoA or cycloheptanecarboxyl-CoA [41,42]. These unique KASIII showed that substrate flexibility on many kinds of acyl-CoA [43]. The specific activity of KASIII from

Alicyclobacillus acidocalderius (aaKASIII) for the reaction between 3HB-CoA and malonyl-ACP is 3-fold higher than that for the reaction between acetyl-CoA and malonyl-ACP [43]. This feature of aaKASIII is good for 3HB-CoA as a substrate. For 3HB-CoA biosynthesis, PhaAB from *Cupriavidus necator* H16 (CPhaAB) is one of the best enzymes in *Synechocysitis*. In previous studies, CPhaAB showed much higher activity than other enzymes for overproduction of PHB or 3-hydroxybutyrate in engineered cyanobacteria and did not show growth inhibition [30,33]. An engineered *E. coli* strain, with the promiscuous KASIII and 3HB-CoA synthesis pathway, produces ω1HFAs [43]. Thus, we adapted this strategy for the production of HFAs in *Synechocystis*.

2. Materials and Methods

2.1 Organisms and Culture Conditions

In this study, a glucose-tolerant strain of *Synechocystis* [44] was used as the wild-type strain. *Synechocystis* cells were grown in BG11 medium [45] buffered with 20 mM 4-(2-hydroxyethyl)-1-piperazineethanesulfonic acid (HEPES)–NaOH (pH 7.5) at 34 °C under continuous illumination by white fluorescent lamps and aerated with 1% (v/v) CO_2-enriched air [46]. Fifty milliliters of cultures were used to measure growth, fatty acid compositions, and mixotrophic culture, and 500 mL of cultures were used for simultaneous measurement of ω1HFAs and photosynthetic parameters.

To screen the transformants and maintain the *Synechocystis* cells, we used BG11 medium solidified with 1.5% (w/v) Bacto-agar (BD Biosciences Japan, Tokyo, Japan), including 25 μg mL^{-1} kanamycin sulfate or chloramphenicol (Fujifilm Wako Pure Chemical, Osaka, Japan), depending on the selection markers. An *E. coli* strain JM109 [47] was grown in

1.8 mL of LB medium [48] at 37 °C with shaking at 180 rpm. All transformants of *E. coli* were maintained on LB medium solidified with 1.5% (w/v) Bacto-agar in the presence of 100 μg mL^{-1} sodium ampicillin (Fujifilm Wako Pure Chemical) and 50 μg mL^{-1} kanamycin sulfate or chloramphenicol, depending on the selection markers.

For DNA extraction, *Cupriavidus necator* H16 was cultivated on medium of Trypot-soya agar (Nissui Pharmaceutical) at 30 °C. *Alicyclobacillus acidocalderius* subsp. *acidocalderius* was cultivated on bacillus acidocalderius medium at 55 °C [49].

2.2 Plasmid Construction and Transformation

The scheme for constructing plasmids in this study is summarized in **Figure 1**. To express the heterologous promiscuous KASIII gene and knockout the *fabH* gene, which encodes a native KASIII in *Synechocystis*, we constructed a plasmid, pMD19Δ*fabH::aaKASIII*. I performed PCR to amplify a DNA fragment containing *aaKASIII* using the chromosomal DNA of *Alicylobacillus acidocalderius* subsp. *acidocalderius* JCM 5260^T (RIKEN BRC, Ibaraki, Japan) as the template and the primer set aaKASIII_F and aaKASIII_R (**Table 2**). After digestions of pTC2031 [37] and the amplified fragment containing the aaKASIII gene with *Nde*I and *Bgl*II, we constructed pTC2031_aaKASIII by ligation. The genomic fragments corresponding to the *fabH* gene were amplified by PCR using *Synechocystis* chromosomal DNA as the template and primer sets fabH_up_F and fabH_dn_R. The amplified DNA fragment was subcloned into a T-vector pMD19 simple vector (Takara Bio, Kusatsu, Japan) to obtain the plasmid pMD19_fabH. To obtain plasmid pMD19Δ*fabH::aaKASIII*, pMD19_*fabH* was linearized by PCR using the primer set fabH_in_F and fabH_in_R, and ligated with the *CmR-Pcpc-aaKASIII* fragment using pTC2031_aaKASIII plasmid as the template and

primer set CmCK_inf_F and CmCK_inf_R using the In-Fusion® HD cloning kit (Takara Bio).

To construct pMD19Δ*phaC*, which is used to knock out the *phaC* gene for PHB polymerase, we performed PCR to amplify a DNA fragment containing *phaC* using *Synechocystis* chromosomal DNA as the template and the primer set phaC_up_F and phaC_dn_R. The amplified DNA fragment was subcloned into a T-vector pMD19 simple vector to obtain the plasmid pMD19*_phaC*. To obtain plasmid pMD19 Δ *phaC*, pMD19*_phaC* was linearized by PCR using the primer set phaC_in_F and phaC_in_R, and circularized with the DNA fragments corresponding to the kanamycin-resistance gene cassette, EZ-Tn5 < KAN-2 > Tnp Transposome Kit (Epicenter, Madison WI) using primer sets Kam_inf_F and Kam_inf_R with the In-Fusion® HD cloning kit.

To construct pMD19*_ΔphaC::SphaAB* for overexpression of the *phaAB* gene from *Synechocystis* and knockout the *phaC* gene in *Synechocystis*, we performed PCR to amplify a DNA fragment containing *phaAB* using *Synechocystis* chromosomal DNA as the template and the primer sets phaAB_up_F and phaAB_dn_R. After digestion of pTC2031 and the amplified fragment containing *SphaAB* with *Nde*I and *Bgl*II, we constructed pTC2031*_SphaAB* by ligation. To construct pMD19*ΔphaC::SphaAB*, pMD19*ΔphaC* was linearized by PCR using primer sets pMD19_Km_PhaC_in_F and pMD19_Km_PhaC_in_F, and ligated with the DNA fragment *Pcpc-phaAB* using pTC2031*_SphaAB* as the template and the primer set cpc_phaAB_inf_F and cpc_phaAB_inf_R with the In-Fusion® HD cloning kit.

To construct pMD19Δ*phaC::CphaAB,* which is a plasmid for overexpression of the heterologous *phaAB* genes from *Cupriavidus necator* H16 (RIKEN BioResource Center) at the *phaC* locus by homologous recombination, pMD19Δ*phaC::SphaAB* was linearized

by PCR using primer sets pMD19_Km_PhaC_in_F and cpc560_R, and ligated with the *CphaAB* fragment using *C. necator* H16 chromosomal DNA as the template and the primer sets CphaAB_inf_F and CphaAB_inf_R by the In-Fusion® HD cloning kit.

To construct pTC2031-S_sodB, that is a plasmid for overexpression of the *sodB* gene from *Synechocystis* at the *slr2031* locus by homologous recombination, pTC2031-S [37] was linearized by PCR using primer set pTCS_Sp_up_F and cpc560_R, and ligated with the *sodB* fragment using *Synechocystis* chromosomal DNA as the template and the primer set sodB_inf_F and sodB_inf_R by the In-Fusion® HD cloning kit.

The DNA sequences of the inserts were confirmed using BigDye® Terminator v.3.1 (Life Technologies, Foster City, CA, USA) and ABI 3130 Genetic Analyzer (Life Technologies).

2.3 Fatty Acid Analysis

The FA profiles of *Synechocystis* transformants were examined using the methods described in our previous studies [37,38,50]. Cells were precipitated by centrifugation, resuspended in 2 mL of methanol, and transferred to glass test tubes. After thorough drying using a concentrating centrifuge (CC-105, Tomy Seiko, Tokyo, Japan), the residue was resuspended in 0.1 M hydrochloric acid methanolic solution (Fujifilm Wako Pure Chemical). The tubes were tightly capped and incubated at 100 °C for 1 h to allow for methyl esterification of the acyl groups in the lipids and conversion into fatty acid methyl esters (FAMEs). The resulting FAMEs were extracted using *n*-hexane. The recovered hexane phases were evaporated, and the residues containing FAMEs were dissolved in 100 μL of acetonitrile and trimethylsilylated by adding 100 μL of *N*, *O*-bis(trimethylsilyl)acetamide: pyridine (1:1), and heated at 90 °C for 30 min. The

trimethylsilylation of the hydroxy group in the acyl group contributes to the separation of FAMEs by decreasing the evaporation temperature and easily identifying the fragmentation of FAMEs [51,52]. To identify FAMEs, we performed gas chromatography (GC) using a GC-2010 gas chromatograph equipped with a QP-2010 mass spectrometer (Shimadzu, Kyoto, Japan). Helium was used as a carrier gas at a constant flow rate of 1.25 mL min^{-1} in split-less mode. A CP-Sil5 CB column (Agilent Technologies, Santa Clara, CA, USA) was used at the following temperatures: 60 °C for 1.5 min, followed by 130 °C at a rate of 20 °C min^{-1}, and then a further increase to 230 °C at a rate of 4 °C min^{-1}.

2.4 Separation of Lipid Classes

To analyze FAs attached to each lipid, the harvested cells were dried using a freeze dryer, and the lipids were extracted with $CHCl_3$: methanol (2:1, v/v). The cell debris was sedimented by centrifugation. The resulting supernatant was transferred into new tubes and evaporated. Then, the samples were resuspended in 500 μL of $CHCl_3$:methanol (2:1, v/v) and applied to a silica gel plate (silica gel 70 FM TLC Plate- Wako, 20 cm × 20 cm; Fujifilm Wako Pure Chemical) washed with $CHCl_3$:methanol (1:1, v/v). Lipids were separated by thin-layer chromatography using acetone:toluene:water (91:30:8, v/v/v). In particular, when plenty of lipids were applied on the thin-layer chromatography (TLC) plates to improve the separation of lipid species, we repeated the development of the solvent at most three times. The lipids were stained with primulin, and the silica gel corresponding to the lipid spots was then scraped off and extracted as described above. To identify the head group of lipid X, the TLC plate was visualized with α-naphthol [53]. The lipids on the TLC plate were stained by spraying 0.2 M α-naphthol in ethanol: 75%

(w/v) H_2SO_4aq (4:11, v/v) and heated at 120 °C for 10 min [54].

2.5 Liquid Chromatography-Mass Spectrometry

For LC/MS analysis, HPLC separation was carried out using a Prominence XR (Shimadzu). The sample was analyzed using L-column2 ODS Nonmetallic frits (2 mm I.D. × 50 mm, 3 μm, Chemical Evaluation and Research Institute, Tokyo, Japan). The liquid separation phases were prepared by mixing three solvents. Solvents A, B, and C were 1 mM ammonium formate, acetonitrile, and 1 mM ammonium formate in 2-propanol, respectively. The gradient profile was as follows: (i) initial 60% A + 38% B + 2% C; (ii) 30 min linear gradient to 2% A + 10% B + 88% C; (iii) 38 min isocratic; (iv) 38.1 min 60% A + 38% B + 2% C; and (v) 41.0 min isocratic. The flow rate was 0.3 mL min^{-1}, and the column temperature was 40 °C. The injection volume was 3 μL. An LTQ Orbitrap XL (Thermo Fisher Scientific) mass spectrometer was operated in both positive and negative ion modes with electrospray ionization source in the range of *m/z* 140−2000. Xcalibur ver. 2.1.0 (Thermo Fisher Scientific) was used to process and analyze the data.

2.6 Measurement of Photosynthetic Activities

Chlorophyll was extracted in 90% methanol and calculated by measuring the absorbance at 665 nm [55]. The oxygen evolution rate of intact cells was measured with a Clark-type oxygen electrode (Oxytherm System, Hansatech Instruments, Norfork, UK). Cells were suspended in BG-11 medium containing 20 mM $NaHCO_3$, and photosynthetic activity in the samples was measured at a light intensity of 300 μmol photons m^{-2} s^{-1}, which represented saturated light conditions. The photosynthetic yield of PSII was determined by measuring the F_V/F_m ratio using an AquaPen fluorometer (AP 100, Photon

Systems Instruments, Drásov, Czech). Samples were dark-adapted for 5 min before measurement.

3 Results

3.1 Construction of the hydroxy fatty acid synthetic pathway and analysis of the fatty acids in transformants

To introduce 3HB-CoA into the FA synthesis (FAS) pathway in *Synechocystis* cells, we utilized a substrate-variable β-keto-acyl-(acyl carrier protein) synthase III (KASIII), which catalyzes the condensation of acetyl-CoA and malonyl-ACP at the first reaction of the FAS pathway. KASIII from *A. acidocalderius* (aaKASIII) has a very wide substrate specificity [43], which can react with many types of acyl-CoA, e.g., propionyl-CoA, isobutyryl-CoA, and benzoyl-CoA, as substrates instead of acetyl-CoA. *E. coli* transformants, which express the aaKASIII and 3HB-CoA biosynthetic gene cluster, produced ω1HFAs [43] (**Figure 2**). *Synechocystis* can synthesize 3HB-CoA, which is a precursor of PHB for carbon storage. To incorporate 3HB-CoA synthesized in *Synechocystis* cells into the FAS pathway, the *fabH* gene encoding the native KASIII of *Synechocystis* was replaced with the aaKASIII gene which was expressed by cpc560 promoter. *A. herbarius* produce ω-cycloheptyl fatty acid which have larger chemical structure at ω-position than ω-cyclohexyl fatty acid have *A. acidocalderius*. KASIII of *A. herbarius* (ahKASIII) might have potential of higher substrate flexibility than of *A. acidocalderius.* Therefore I attempted to construct *Synechocystis*Δ*fabH*::*ahKASIII* strain. But I could not obtain the transformant. The *Synechocystis*Δ*fabH*::Pcpc-*aaKASIII* strain (*aaKASIII*+) cultivated under the photoautotrophic condition with the standard BG-11

medium [45] for 7 d. GC-MS analysis revealed that the transformant under the standard BG-11 condition contained no ω1HFAs. I speculated that the 3HB-CoA pool in *Synechocystis* cells cultivated under standard BG-11 conditions was insufficient to synthesize ω1HFAs because of the low PHB accumulation, i.e., approximately 1%−5% (w/w) of dry cells. To enhance the 3HB-CoA biosynthesis, I cultivated the cells in the phosphate-limiting conditions with 4% acetate, in which conditions the PHB productivity is increased up to 28.8% (w/w) of the dry cells [31]. However, in the photomixotrophic conditions, the FA composition extracted from the transformant showed no ω1HFAs (data not shown). To confirm whether the cpc promoter works under phosphate deficiency with acetate condition, *Synechocystis* having aaKASIII+ gene expressed by trc promoter (*Synechocystis*Δ*fabH*::Ptrc-*aaKASIII*) constructed. But this strain also didn't produce ω1HFAs.

To increase the content of 3HB-CoA, two additional genetic modifications were employed. First, the ability of PHB polymerization was deleted because PHB synthesized from 3HB-CoA should compete with ω1HFA biosynthesis. Because PHB biosynthesis from 3HB-CoA is catalyzed by PHB polymerase encoded by the *phaC* and *phaE* genes, we inactivated the *phaC* gene to enhance the accumulation of 3HB-CoA, the ω1HFA precursor. Second, we overexpressed *phaA* and *phaB* (*phaAB*) genes by substituting with the *phaC* gene in the cells of *aaKASIII*+. These two gene products are involved in the biosynthesis of 3HB-CoA, PhaA catalyzes the condensation of two acetyl-CoA molecules to yield acetoacetyl-CoA, and PhaB then reduces it to 3HB-CoA. In addition to *Synechocystis*Δ*fabH*::*aaKASIII*, we constructed two other transformants, Δ*phaC* (*aaKASIII*+/*phaC*-), *Synechocystis*Δ*fabH*::*aaKASIII*, Δ*phaC*::*SphaAB* (*aaKASIII*+/*phaC*-/*SphaAB*+). However, ω1HFAs were not detected in either

aaKASIII+/*phaC-* and *aaKASIII+*/*phaC-*/*SphaAB+* cells cultivated in the standard BG-11. To enhance 3HB-CoA biosynthesis, we cultivated *aaKASIII+*, *aaKASIII+*/*phaC-,* and *aaKASIII+*/*phaC-*/*SphaAB+* cells under phosphate-limiting conditions with 4% acetate, and PHB productivity was increased up to 28.8% (w/w) of the dry cells [31]. However, under photomixotrophic conditions, the FA composition extracted from these transformants showed no ω1HFAs (data not shown). Expression of additional genes by trc promoter instead of cpc promoter attempted, but these strains also contained no ω1HFAs.

To further increase 3HB-CoA biosynthesis, we attempted to express the exogenous *phaAB* genes in *Synechocystis*. There were two candidates of genes, one is *phaAB* from *C. necator* H16 and another is *nphT7* which encode acetoacetyl-CoA synthase driven by ATP from *Streptomyces* sp. (strain CL190) with *phaB* from *C. necator* H16. In the previous study [43], PhaA and PhaB from *C. necator* H16 had much higher activity than those of *Synechocystis*. NphT7 is also a good candidate to increase the 3HB-CoA pool because acetoacetyl-CoA synthesis by NphT7 is an irreversible reaction while the synthesis by PhaA is a reversible reaction. I attempted to introduced the *phaAB* genes of *C. necator* H16 or codon optimizing nphT7 (**Figure 3**) with *phaB* from *C. necator* H16 into the *phaC* region of *Synechocystis*Δ*fabH*::*aaKASIII* strain to obtain *Synschocystis*Δ*fabH*::*aaKASIII*, Δ*phaC*::*CphaAB* (*aaKASIII+*/*phaC-*/*CphaAB+*) or *Synschocystis*Δ*fabH*::*aaKASIII*, Δ*phaC*::*nphT7-CphaB* (*aaKASIII+*/*phaC-*/*nphT7-CphaAB+*) cells. I could obtain the *aaKASIII+*/*phaC-*/*CphaAB+* but not *aaKASIII+*/*phaC-*/*nphT7-CphaAB+*. Total lipids were extracted from the *aaKASIII+*/*phaC-*/*CphaAB+* cells cultivated under standard BG-11 conditions with 70 μmol photons m^{-2} s^{-1} illumination, and then trans-esterified and trimethylsilylated. The

total ion chromatogram of FAMEs from the *aaKASIII+/phaC-/CphaAB+* cells showed three additional peaks, **1**, **2**, and **3**, with retention times of 25.1, 28.5, and 29.2 min, respectively, compared to that of wild-type cells (**Figure 4A**). As the canonical ω1HFAs were not commercially available, we had to identify them from the fragment patterns by GC/MS analyses. The fragmented ions from the three peaks contained a characteristic ion with *m/z* 117, which represents the resultant ions from the ω1HFAs by α cleavage. Peaks 1, 2, and 3 also contained fragment ions, whose *m/z* corresponded to the loss of the ω methyl and methoxy groups (**Figure 5**). The mass spectrometry of the three peaks corresponded to those of previous studies [43,56]. I determined that the three species of ω1HFAs were 15-hydroxyhexadecanoic acid (16:0 OH), 17-hydroxyoctadecanoic acid (18:0 OH), and 17-hydroxyoctadec-9-enoic acid (18:1 OH) (Figure 4B and 5). These ω1HFAs might be chiral compounds because 3HB-CoA synthesized by PhaAB from *C. necator* H16 is (*R*)-3-hydroxybutyryl-CoA [33]. The ω1HFAs content was about 2.1 mol% of total FAs (**Figure 4B**). Interestingly, lipids in the *aaKASIII+/phaC-/CphaAB+* cells contained a high amount of 18:0, while decreasing the content of 18:2 and 18:3. At this moment, we do not know about the relationship between ω1HFA production and unsaturation alteration of C18 FAs. These results indicated that the higher enzyme activity of PhaAB from *C. necator* H16 allowed the synthesis of ω1HFAs in the engineered *Synechocystis* cells expressing the aaKASIII, which can catalyze 3HB-CoA as a substrate.

3.1 Effect of Hydroxy Fatty Acid Production on Growth and Photosynthesis.

Although all other strains constructed in this study grew as well as the wild-type under continuous illumination with 70 μmol photons m^{-2} s^{-1}, the growth of *aaKASIII+/phaC-/CphaAB+* cells was retarded. Interestingly, *aaKASIII+/phaC-/CphaAB+* cell growth

under 35 μmol photons m^{-2} s^{-1}, was similar to that of wild-type cells (**Figure 6**). However, under low-light conditions, *aaKASIII+*/*phaC-*/*CphaAB+* cells accumulated only a small amount of ω1HFAs (i.e., 0.04 mol%), which was much lower than that of cells grown under 70 μmol photons m^{-2} s^{-1} (**Figure 7**). These results demonstrated the correlation between growth and ω1HFA biosynthesis in *Synechocystis* cells.

To investigate the relationship between ω1HFA production and photosynthesis, we simultaneously measured ω1HFA contents, photosynthetic activity, chlorophyll content, and photosynthetic yield of photosystem II (PSII) in the cells cultured under various light conditions, i.e., 35, 70, or 140 μmol photons m^{-2} s^{-1}, for 48 h. As a control, wild-type cells were cultivated under 140 μmol photons m^{-2} s^{-1} (**Figure 8**). These measurements showed three important findings regarding the relationship between ω1HFA production and photosynthesis. First, the higher light intensity of cultivation stimulated ω1HFA accumulation in *Synechocystis* cells. Second, ω1HFA accumulation started in the early stage of cultivation. As high light intensity promoted the accumulation of acetyl-CoA, which stimulated 3HB-CoA biosynthesis, ω1HFAs contents in *aaKASIII+*/*phaC-*/*CphaAB+* cells grown under 70 and 140 μmol photons m^{-2} s^{-1} rapidly increased within 6 h, while that of the cells cultivated at 35 μmol photons m^{-2} s^{-1} accumulated slowly (**Figure 8A**). In particular, cells in the low cell density in the early stage of cultivation effectively absorbed photons and synthesized 3HB-CoA via acetyl-CoA biosynthesis. Third, ω1HFA accumulation in the early stage of cultivation inhibited photosynthesis activity under high light intensity. Under 140 μmol photons m^{-2} s^{-1}, photosynthetic parameters of *aaKASIII+*/*phaC-*/*CphaAB+* cells, i.e., chlorophyll content and quantum yield, Fv/Fm, continuously decreased after cultivation. In comparison, they maintained their initial levels under 35 and 70 μmol photons m^{-2} s^{-1}, with wild-type cells as a control (**Figure 8B**

and **C**). These changes in photosynthetic parameters suggested that ω1HFA accumulation in the early stage of cultivation promoted the inactivation of photosynthetic activity, i.e., photoinhibition. Under 140 μmol photons m^{-2} s^{-1}, *aaKASIII+*/*phaC-*/*CphaAB+* photosynthetic activity also dropped after 12 h and reached 26 μmol O_2 mg Chl^{-1} h^{-1} at 48 h. Meanwhile, under 35 μmol photons m^{-2} s^{-1}, it was maintained at approximately 60 μmolO_2 mg Chl^{-1} h^{-1} until 48 h (**Figure 8D**). *aaKASIII+*/*phaC-*/*CphaAB+* cells incubated under 70 μmol photons m^{-2} s^{-1} and wild-type cells incubated under 140 μmol photons m^{-2} s^{-1} for 48 h reached approximately 50 and 60 μmolO_2 mg Chl^{-1} h^{-1}, respectively, owing to the apparent decrease in light intensity by self-scattering caused by the increase in cell density (**Figure 8D** and **Figure 9**). ω1HFA production in *aaKASIII+*/*phaC-*/*CphaAB+* cells incubated under 140 μmol photons m^{-2} s^{-1} reached 1.5 ± 1.3 mol% in total FAs at 24 h. These results indicate that ω1HFAs production, i.e., accumulation of membrane lipids esterified the ω1HFAs, caused a reduction in growth rate and photosynthetic activity.

3.2 Production of hydroxy fatty acids under mixotrophic conditions

To enhance ω1HFA production, *aaKASIII+*/*phaC-*/*CphaAB+* cells were cultivated for 1 day under mixotrophic conditions by addition of 10 mM glucose as a carbon source into BG-11 with continuous illumination at 140 μmol photons m^{-2} s^{-1}, and the initial cell density OD_{730} was 1.0 to protect the cells from inactivation of photosynthesis by high light intensity. Under this mixotrophic condition, *aaKASIII+*/*phaC-*/*CphaAB+* cells died, while under autotrophic conditions, the cells could survive and accumulated 1.9 mol% ω1HFA. Under heterotrophic conditions, i.e., cultured in the dark and adding 10 mM glucose, *aaKASIII+*/*phaC-*/*CphaAB+* cells could grow slowly but accumulated undetectable levels of ω1HFA (data not shown). I hypothesized that the

aaKASIII+/*phaC-*/*CphaAB+* transformant deleted the ability to synthesize PHB as a storage compound; therefore, catabolism of glucose decreased, and the extra glucose might inhibit cell growth.

3.3 Lipid composition of the ω1HFA producing transformant

The simultaneous measurement of ω1HFAs production and photosynthetic parameters indicated that ω1HFAs depressed photosynthesis. To understand the inactivation of photosynthesis by ω1HFAs in *aaKASIII+*/*phaC-*/*CphaAB+* cells, we measured ω1HFAs accumulation in each lipid class from *aaKASIII+*/*phaC-*/*CphaAB+* cells to analyze membrane lipids of the cells. Lipids were extracted from the wild-type and *aaKASIII+*/*phaC-*/*CphaAB+* cells and separated by TLC. Cyanobacteria have four classes of membrane lipids: MGDG, DGDG, sulfoquinovosyldiacylglycerol (SQDG), and phosphatidyldiacylglycerol (PG). Table 1 shows the FA compositions of all lipid classes from *aaKASIII+*/*phaC-*/*CphaAB+* cells, which were cultivated for 24 h under 70 μmol photons m^{-2} s^{-1} and accumulated 1.3 mol% ω1HFAs, with wild-type cells as a control. Total ω1HFAs in SQDG and PG extracted from the *aaKASIII+*/*phaC-*/*CphaAB+* cells were 0.8 and 0.9 mol%, respectively. The introduction of ω1HFAs into PG could explain the effect of ω1HFAs on photosynthetic activity and altering the growth rate because PG is directly bound to the photosystems and has a specific role in electron transport [57,58]. In particular, the hydroxy group of the ω1HFAs on PG, which is deeply buried in the reaction center of PSII, might be oxidized and cause structural disorder of PSII. The photosystem affected by ω1HFA stimulates the production of reactive oxygen species that are toxic to the cells. To reduce ROS in the *aaKASIII+*/*phaC-*/*CphaAB+* cells, we overexpressed the native superoxide dismutase which is a ROS quenching enzyme

encoded by *sodB* gene [59,60]. This *aaKASIII+/phaC-/CphaAB+/sodB+* strain grew better than *aaKASIII+/phaC-/CphaAB+* strain (**Figure 10**), although *aaKASIII+/phaC-/CphaAB+/sodB+* strain produced same ratio of ω1HFA with *aaKASIII+/phaC-/CphaAB+* strain under 140 μmol photons m^{-2} s^{-1}. The decrease in Fv/Fm observed in *aaKASIII+/phaC-/CphaAB+* cells cultivated under 140 μmol photons m^{-2} s^{-1} was consistent with this hypothesis (**Figure 8B**). Although galactolipids MGDG and DGDG were recovered from the TLC plates, they contained a small amount of ω1HFAs. Total lipids extracted from *aaKASIII+/phaC-/CphaAB+* cells showed an additional spot migrated under the spot of MGDG on the TLC plate, referred to as lipid X (**Figure 11**). Visualization of lipid X on the TLC plate by α-naphthol turned the spot of the lipid into yellow, indicating that the head group of lipid X might be a saccharide (**Figure 12**). These staining results of lipid X on the TLC plate indicated that lipid X might be an MGDG analog.

To understand the small amount of ω1HFAs in galactolipids, we attempted to determine the molecular structure of lipid X by liquid chromatography coupled with mass spectrometry (LC/MS). I confirmed that lipid X included at least five species of galactolipids esterifying ω1HFA by the fragmentation pattern of LC/MS analyses, with the positive and negative ionization modes. The chromatogram of lipid X with the positive ionization mode indicated that lipid X was the mixture of at least five forms of lipids, which were separated at 19.25, 20.07, 21.06, 21.57, and 22.23 min, designated as peak No. **1**, **2**, **3**, **4**, and **5**, respectively (**Figure 11B** and **Figure 13**). As seen in **Table 5**, the mass spectra of these five lipids showed that all of them possessed major peaks between *m/z* 791.52 and 797.57, and minor peaks between *m/z* 807.50 and 813.54. The former might correspond to the parent lipid ionized with a sodium ion, $[M+Na]^+$, and the

latter indicated potassium ionized from $[M+K]^+$. These peaks also contained five fragment ions, designated as **a**, **b**, **c**, **d**, and **e**, whose cleavage patterns are shown in **Figure 11D** and, **Figure 13A** and **B**. Fragmentation was estimated from the reference MS data of MGDG from previous studies [61–63]. Structure estimation for the five lipid forms from the mass spectrum indicated that peaks No. **1**, **2**, **3**, **4**, and **5** were glycerolipids with a hexose ($C_6H_{12}O_6$) moiety as a headgroup, an ω1HFA, and either a saturated or unsaturated FA. The FA pairs of lipids, **1**, **2**, **3**, **4**, and **5** were estimated as 16:0 OH/18:3, 16:0 OH/18:2, 16:0 OH/18:1, 16:0/18:1 OH, 16:0 OH/18:0 OH, respectively (**Table 5**). In the negative ionization mode, three forms of lipids were observed in lipid X, which were eluted at 19.78, 20.77, and 21.29 min. Each mass spectrum showed two ions with m/z values corresponding to $[M+HCOO]^-$ and $[M-H]^-$ ions of the molecules identified as No. **2**, **3,** and **4** by the positive ionization mode (**Figure 14**). LC/MS characterization results for lipid X indicated that this novel lipid might be MGDG containing at least one ω1HFA moiety and either C16 or C18 FA, as generally existing in *Synechocystis* cells. The lower mobility in lipid X than in MGDG on the TLC plates might be caused by the higher possibility of hydrogen bond formation between a hydroxy group of the ω1HFA and silanol group (-Si-OH) on the TLC plate. This lower mobility of lipid X might also cause a lower ω1HFA ratio in galactolipids, i.e., MGDG and DGDG, than that in SQDG and PG. LC/MS analysis revealed that lipid X might possess a 1:1 molecular ratio of ω1HFAs and standard FAs. These results indicated that MGDG in *aaKASIII+*/*phaC-*/*CphaAB+* cells also contained ω1HFA. The introduction of 16:0 OH into the sn-2 position of lipids showed that MGDG contained a ω1HFAs ratio similar to that of PG and SQDG because FA at the sn-2 position is common to all lipid classes in *Synechocysitis*.

4 Discussion

I succeeded to construct the ω1HFA-producing cyanobacterial strain which expresses the promiscuous KASIII from *A. acidocalderius* by substitution of the native KASIII gene and the exogenous PhaAB from *C. necator* H16 by substitution of the PHB synthetase gene. This transformant produced 2.1 mol% of the ω1HFAs in the total FAs under the illumination of 70 μmol photons m^{-2} s^{-1}. In this condition, this transformant showed growth inhibition. Whereas under 35 μmol photons m^{-2} s^{-1}, growth of the mutant strain recovered up to almost the same level of the wild-type strain. From the time course experiment of relationship between ω1HFAs ratio and photosynthetic parameters such as photosynthetic activity, quantum efficiency of PSII and chlorophyll content indicated that ω1HFA production inhibited the photosynthesis of *Synechocystis*. The lipid analysis of the mutant showed that galactoglycerolipids, which are MGDG and DGDG, contained a significantly smaller amount of ω1HFAs than other lipids and a novel spot appeared on TLC analysis which contained ω1HFAs.

The ω1HFAs production affects photosynthesis on cyanobacteria due to the introduction of ω1HFAs into PG directly bound with the photosystem. The undesired chemical reaction might occur on the hydroxy group of ω1HFAs on the photosystem caused by strong oxidation or reducing power of the photosystem. In the previous study, FFA production for biofuel in cyanobacteria inhibited the growth of cyanobacteria due to toxicity of FFA in the cell [34]. To improve the growth inhibition and productivity of FFA in the strain, superoxide dismutase which is the enzyme for break down the reactive oxygen species in the cell is overexpressed. If I apply this strategy to the ω1HFAs-producing strain, ω1HFAs productivity might improve. Cyanobacterial lipids are only

utilized as membrane components so ω1HFAs strongly affect the cell. If eukaryotic microalgae which produce triacylglycerol as storage compounds such as green algae or diatom is used as cell substrate, production of ω1HFAs might improve. In the previous study, the growth rate of engineered diatom, which produces 12-hydroxyoctadec-9-enoic acid (ricinoleic acid) is similar with wild-type strain because esterification between hydroxy group on ricinoleic acid and carboxyl croup on standard FAs naturally happen and this might provide detoxication of hydroxy group in the diatom cells [20]. This esterification naturally occurs in the diatom, so this biological feature is suited for ω1HFAs.

In my study showed that the galactolipid containing ω1HFAs easily separated by TLC, it has the potential to be a novel chemical compound such as antibacterial and antivirus biosurfactant like sophorolipid [64]. ω1HFAs also has the potential as a chemical feedstock. In the previous study, ω1HFAs derived from sophorolipid secreted by *Candida bombicola* showed potential as a lubricant [65]. However, the photoautotrophic production of ω1HFAs is not efficient in this study. Thus ω1HFAs productivity should improve to characterize the potential of ω1HFAs and lipids containing ω1HFAs as feedstock.

Acknowledgements

I would like to express my gratitude to Professor Iwane Suzuki for his appropriate guidance and supervision in my study life.

I am also grateful to Professor Masashi Kijima, Associate Professor Koichiro Awai in Shizuoka University, Dr. Hirotoshi Endo, Dr. Shuntaro Machida, and Dr. Bakku Ranjith Kumar for their experimental support and helpful suggestions.

Special thanks must be given to all members of the Laboratory of Regulation of Photosynthetic Metabolism of the University of Tsukuba.

Reference

[1] U. Biermann, W. Friedt, S. Lang, W. Lühs, G. Machmüller, J.O. Metzger, M.R. Mark, H.J. Schäfer, M.P. Schneider, New syntheses with oils and fats as renewable raw materials for the chemical industry, Angew Chemie Int Ed. 39 (2000) 2206–2224. https://doi.org/10.1002/9783527619849.ch25.

[2] K.R. Kim, D.K. Oh, Production of hydroxy fatty acids by microbial fatty acid-hydroxylation enzymes, Biotechnol Adv. 31 (2013) 1473–1485. https://doi.org/10.1016/j.biotechadv.2013.07.004.

[3] A. V. Rawlings, Trends in stratum corneum research and the management of dry skin conditions, Int J Cosmet Sci. 25 (2003) 63–95. https://doi.org/10.1046/j.1467-2494.2003.00174.x.

[4] A. Abe, K. Sugiyama, Growth inhibition and apoptosis induction of human melanoma cells by ω-hydroxy fatty acids, Anticancer Drugs. 16 (2005) 543–549. https://journals.lww.com/anti-cancerdrugs/Abstract/2005/06000/Growth_inhibition_and_apoptosis_induction_of_human.10.aspx.

[5] C. Liu, F. Liu, J. Cai, W. Xie, T.E. Long, S.R. Turner, A. Lyons, R.A. Gross, Polymers from fatty acids: Poly(ω-hydroxyl tetradecanoic acid) synthesis and physico-mechanical studies, Biomacromolecules. 12 (2011) 3291–3298. https://doi.org/10.1021/bm2007554.

[6] M. Schrewe, A.O. Magnusson, C. Willrodt, B. Bühler, A. Schmid, Kinetic analysis of terminal and unactivated C-H bond oxyfunctionalization in fatty acid methyl esters by monooxygenase-based whole-cell biocatalysis, Adv Synth Catal. 353 (2011) 3485–3495. https://doi.org/10.1002/adsc.201100440.

[7] F. Pinot, Cytochrome P450 metabolizing fatty acids in living organisms, FEBS J. 278 (2011) 181–181. https://doi.org/10.1111/j.1742-4658.2010.07946.x.

[8] I.N.A. Van Bogaert, S. Groeneboer, K. Saerens, W. Soetaert, The role of cytochrome P450 monooxygenases in microbial fatty acid metabolism, FEBS J. 278 (2011) 206–221. https://doi.org/10.1111/j.1742-4658.2010.07949.x.

[9] H.A. Park, G. Park, W. Jeon, J.O. Ahn, Y.H. Yang, K.Y. Choi, Whole-cell biocatalysis using cytochrome P450 monooxygenases for biotransformation of sustainable bioresources (fatty acids, fatty alkanes, and aromatic amino acids), Biotechnol Adv. (2020) 107504. https://doi.org/10.1016/j.biotechadv.2020.107504.

[10] M. Pawar, A. Kadam, O. Yemul, V. Thamke, K. Kodam, Biodegradable bioepoxy resins based on epoxidized natural oil (cottonseed & algae) cured with citric and tartaric acids through solution polymerization: A renewable approach, Ind Crops Prod. 89 (2016) 434–447. https://doi.org/10.1016/j.indcrop.2016.05.025.

[11] Z.S. Petrović, X. Wan, O. Bilić, A. Zlatanić, J. Hong, I. Javni, M. Ionescu, J. Milić, D. Degruson, Polyols and polyurethanes from crude algal oil, JAOCS, J.

Am. Oil Chem. Soc. 90 (2013) 1073–1078. https://doi.org/10.1007/s11746-013-2245-9.

[12] C. Negrell, A. Cornille, P. de Andrade Nascimento, J.J. Robin, S. Caillol, New bio-based epoxy materials and foams from microalgal oil, Eur J Lipid Sci Technol. 119 (2017) 1–13. https://doi.org/10.1002/ejlt.201600214.

[13] P. Roesle, F. Stempfle, S.K. Hess, J. Zimmerer, C. Ríobártulos, B. Lepetit, A. Eckert, P.G. Kroth, S. Mecking, Synthetic polyester from algae oil, Angew Chemie Int Ed. 53 (2014) 6800–6804. https://doi.org/10.1002/anie.201403991.

[14] A. Katz, J. Weckesser, G. Drews, H. Mayer, Chemical and biological studies on the lipopolysaccharide (O-antigen) of Anacystis nidulans, Arch Microbiol. 113 (1977) 247–256. https://doi.org/10.1007/BF00492032.

[15] J. Weckesser, A. Katz, G. Drews, H. Mayer, I. Fromme, Lipopolysaccharide containing L-acofriose in the filamentous blue-green alga Anabaena variabilis, J Bacteriol. 120 (1974) 672–678.

[16] W. Schmidt, G. Drews, J. Weckesser, H. Mayer, Lipopolysaccharides in four strains of the unicellular cyanobacterium Synechocystis, Arch Microbiol. 127 (1980) 217–222. https://doi.org/10.1007/BF00427196.

[17] G.I. Matsumoto, H. Nagashima, Occurrence of 3-hydroxy acids in microalgae and cyanobacteria and their geochemical significance, Geochim Cosmochim Acta. 48 (1984) 1683–1687. https://doi.org/10.1016/0016-7037(84)90337-5.

[18] P. Blokker, S. Schouten, H. Van Den Ende, J.W. De Leeuw, J.S. Sinninghe Damsté, Cell wall-specific ω-hydroxy fatty acids in some freshwater green microalgae, Phytochemistry. 49 (1998) 691–695. https://doi.org/10.1016/S0031-9422(98)00229-5.

[19] B. Allard, J. Templier, High molecular weight lipids from the trilaminar outer wall (TLS)-containing microalgae Chlorella emersonii, Scenedesmus communis and Tetraedron minimum, Phytochemistry. 57 (2001) 459–467. https://doi.org/10.1016/S0031-9422(01)00071-1.

[20] M. Kajikawa, T. Abe, K. Ifuku, K.I. Furutani, D. Yan, T. Okuda, A. Ando, S. Kishino, J. Ogawa, H. Fukuzawa, Production of ricinoleic acid-containing monoestolide triacylglycerides in an oleaginous diatom, Chaetoceros gracilis, Sci Rep. 6 (2016) 1–13. https://doi.org/10.1038/srep36809.

[21] R. Holic, H. Yazawa, H. Kumagai, H. Uemura, Engineered high content of ricinoleic acid in fission yeast Schizosaccharomyces pombe, Appl Genet Mol Biotechnol. 95 (2012) 179–187. https://doi.org/10.1007/s00253-012-3959-6.

[22] O.K.C. Wolk, Genetic tools for cyanobacteria, Appl Microbiol Biotechnol. 58 (2002) 123–137. https://doi.org/10.1007/s00253-001-0864-9.

[23] D.C. Ducat, J.C. Way, P.A. Silver, Engineering cyanobacteria to generate high-value products, Trends Biotechnol. 29 (2011) 95–103. https://doi.org/10.1016/j.tibtech.2010.12.003.

[24] N.-S. Lau, M. Matsui, A. Al-Ashraf Abdullah, Cyanobacteria: Photoautotrophic microbial factories for the sustainable synthesis of industrial products, Biomed

Res Int. 2015 (2015) 754934. https://doi.org/10.1155/2015/754934.

[25] S.A. Angermayr, A. Gorchs Rovira, K.J. Hellingwerf, Metabolic engineering of cyanobacteria for the synthesis of commodity products, Trends Biotechnol. 33 (2015) 352–361. https://doi.org/10.1016/j.tibtech.2015.03.009.

[26] A.E. Case, S. Atsumi, Cyanobacterial chemical production, J Biotechnol. 231 (2016) 106–114. https://doi.org/10.1016/j.jbiotec.2016.05.023.

[27] Y. Chisti, Biodiesel from microalgae, Biotechnol Adv. 25 (2007) 294–306. https://doi.org/10.1016/j.biotechadv.2007.02.001.

[28] R. Davis, J. Markham, C. Kinchin, N. Grundl, E.C.D. Tan, D. Humbird, Process Design and Economics for the Production of Algal Biomass: Algal Biomass Production in Open Pond Systems and Processing Through Dewatering for Downstream Conversion, 2016. www.nrel.gov/publications. (accessed June 29, 2020).

[29] W. Khetkorn, A. Incharoensakdi, P. Lindblad, S. Jantaro, Enhancement of poly-3-hydroxybutyrate production in Synechocystis sp. PCC 6803 by overexpression of its native biosynthetic genes, Bioresour Technol. 214 (2016) 761–768. https://doi.org/10.1016/j.biortech.2016.05.014.

[30] K. Sudesh, K. Taguchi, Y. Doi, Effect of increased PHA synthase activity on polyhydroxyalkanoates biosynthesis in Synechocystis sp. PCC6803, Int J Biol Macromol. 30 (2002) 97–104. https://doi.org/10.1016/S0141-8130(02)00010-7.

[31] B. Panda, P. Jain, L. Sharma, N. Mallick, Optimization of cultural and nutritional conditions for accumulation of poly-β-hydroxybutyrate in Synechocystis sp. PCC 6803, Bioresour Technol. 97 (2006) 1296–1301. https://doi.org/10.1016/j.biortech.2005.05.013.

[32] W. Khetkorn, A. Incharoensakdi, P. Lindblad, S. Jantaro, Enhancement of poly-3-hydroxybutyrate production in Synechocystis sp. PCC 6803 by overexpression of its native biosynthetic genes, Bioresour Technol. 214 (2016) 761–768. https://doi.org/10.1016/j.biortech.2016.05.014.

[33] B. Wang, S. Pugh, D.R. Nielsen, W. Zhang, D.R. Meldrum, Engineering cyanobacteria for photosynthetic production of 3-hydroxybutyrate directly from CO2, Metab Eng. 16 (2013) 68–77. https://doi.org/10.1016/j.ymben.2013.01.001.

[34] A. Kato, K. Use, N. Takatani, K. Ikeda, M. Matsuura, K. Kojima, M. Aichi, S.I. Maeda, T. Omata, Modulation of the balance of fatty acid production and secretion is crucial for enhancement of growth and productivity of the engineered mutant of the cyanobacterium Synechococcus elongatus, Biotechnol Biofuels. 9 (2016) 91. https://doi.org/10.1186/s13068-016-0506-1.

[35] A.M. Ruffing, Improved free fatty acid production in cyanobacteria with Synechococcus sp. PCC 7002 as host, Front Bioeng Biotechnol. 2 (2014) 17. https://doi.org/10.3389/fbioe.2014.00017.

[36] X. Liu, J. Sheng, R. Curtiss, Fatty acid production in genetically modified cyanobacteria, Proc Natl Acad Sci U S A. 108 (2011) 6899–6904. https://doi.org/10.1073/pnas.1103014108.

[37] S. Machida, I. Suzuki, Characterization of cyanobacterial cells synthesizing 10-methyl stearic acid, Photosynth Res. 139 (2019) 173–183. https://doi.org/10.1007/s11120-018-0537-5.

[38] S. Machida, Y. Shiraiwa, I. Suzuki, Construction of a cyanobacterium synthesizing cyclopropane fatty acids, Biochim Biophys Acta Mol Cell Biol Lipids. 1861 (2016) 980–987. https://doi.org/10.1016/j.bbalip.2016.05.012.

[39] C.E. Drakontis, S. Amin, Biosurfactants: Formulations, properties, and applications, Curr Opin Colloid Interface Sci. 48 (2020) 77–90. https://doi.org/10.1016/j.cocis.2020.03.013.

[40] K.H. Choi, R.J. Heath, C.O. Rock, β-Ketoacyl-acyl carrier protein synthase III (FabH) is a determining factor in branched-chain fatty acid biosynthesis, J Bacteriol. 182 (2000) 365–370. https://doi.org/10.1128/JB.182.2.365-370.2000.

[41] H. Matsubara, K. Goto, T. Matsumura, K. Mochida, M. Iwaki, M. Niwa, K. Yamasato, Alicyclobacillus acidiphilus sp. nov., a novel thermo-acidophilic, ω-alicyclic fatty acid-containing bacterium isolated from acidic beverages, Int. J. Syst. Evol. Microbiol. 52 (2002) 1681–1685. https://doi.org/10.1099/ijs.0.02169-0.

[42] K. Goto, H. Matsubara, K. Mochida, T. Matsumura, Y. Hara, M. Niwa, K. Yamasato, Alicyclobacillus herbarius sp. nov., a novel bacterium containing ω-cycloheptane fatty acids, isolated from herbal tea, Int. J. Syst. Evol. Microbiol. 52 (2002) 109–113. https://doi.org/10.1099/00207713-52-1-109.

[43] S. Garg, L. Rizhsky, H. Jin, X. Yu, F. Jing, M.D. Yandeau-Nelson, B.J. Nikolau, Microbial production of bi-functional molecules by diversification of the fatty acid pathway, Metab Eng. 35 (2016) 9–20. https://doi.org/10.1016/j.ymben.2016.01.003.

[44] J.G.K. Williams, Construction of specific mutations in photosystem II photosynthetic reaction center by genetic engineering methods in Synechocystis 6803, Methods Enzymol. 167 (1988) 766–778. https://doi.org/10.1016/0076-6879(88)67088-1.

[45] R.Y. Stanier, R. Kunisawa, M. Mandel, G. Cohen-Bazire, Purification and properties of unicellular blue-green algae (order Chroococcales)., Bacteriol Rev. 35 (1971) 171–205.

[46] M.N. Wada Hajime, Synechocystis PCC6803 mutants defective in desaturation of fatty acids, Plant Cell Physiol. (1989) 971–978. https://doi.org/10.1093/oxfordjournals.pcp.a077842.

[47] C. Yanisch-Perron, J. Vieira, J. Messing, Improved M13 phage cloning vectors and host strains: nucleotide sequences of the M13mpl8 and pUC19 vectors, Gene. 33 (1985) 103–119. https://doi.org/10.1016/0378-1119(85)90120-9.

[48] G. Bertani, Studies on lysogenesis. I. The mode of phage liberation by lysogenic Escherichia coli., J Bacteriol. 62 (1951) 293–300.

[49] G. Darland, T. Brock, Bacillus acidocaldarius sp.nov., an acidophilic thermophilic spore-forming bacterium, n.d.

[50] T. Kotajima, Y. Shiraiwa, I. Suzuki, Functional screening of a novel Δ15 fatty acid desaturase from the coccolithophorid Emiliania huxleyi, Biochim Biophys Acta Mol Cell Biol Lipids. 1841 (2014) 1451–1458. https://doi.org/10.1016/j.bbalip.2014.07.010.

[51] N. Nicolaides, V.G. Soukup, E.C. Ruth, Mass spectrometric fragmentation patterns of the acetoxy and trimethylsilyl derivatives of all the positional isomers of the methyl hydroxypalmitates, Biol Mass Spectrom. 10 (1983) 441–449. https://doi.org/10.1002/bms.1200100802.

[52] K. Komagata, K.I. Suzuki, 4 Lipid and cell-wall analysis in bacterial systematics, Methods Microbiol. 19 (1988) 161–207. https://doi.org/10.1016/S0580-9517(08)70410-0.

[53] M. Kates, Techniques of lipidology, in: R. Burdon, P. van Knippenberg (Eds.), Lab. Tech. Biochem. Mol. Biol., 2nd ed., American Elsevier, New York, 1986: pp. 347–446. https://doi.org/10.1042/bst0160906.

[54] K. Awai, H. Ohta, N. Sato, Oxygenic photosynthesis without galactolipids, Proc Natl Acad Sci U S A. 111 (2014) 13571–13575. https://doi.org/10.1073/pnas.1403708111.

[55] N.T. de Marsac, J. Houmard, Complementary chromatic adaptation: physiological conditions and action spectra, Methods Enzymol. 167 (1988) 318–328. https://doi.org/10.1016/0076-6879(88)67037-6.

[56] J. Liu, C. Zhang, W. Lu, Biosynthesis of long-chain ω-hydroxy fatty acids by engineered Saccharomyces cerevisiae, J Agric Food Chem. 67 (2019) 4545–4552. https://doi.org/10.1021/acs.jafc.9b00109.

[57] K. Kobayashi, K. Endo, H. Wada, Specific distribution of phosphatidylglycerol to photosystem complexes in the thylakoid membrane, Front Plant Sci. 8 (2017) 1991. https://doi.org/10.3389/fpls.2017.01991.

[58] K. Kobayashi, H. Wada, Role of lipids in chloroplast biogenesis, in: Subcell Biochem., Springer New York, 2016: pp. 103–125. https://doi.org/10.1007/978-3-319-25979-6_5.

[59] Y. Umena, K. Kawakami, J.R. Shen, N. Kamiya, Crystal structure of oxygen-evolving photosystem II at a resolution of 1.9Å, Nature. 473 (2011) 55–60. https://doi.org/10.1038/nature09913.

[60] J. Bhattacharya, K. GhoshDastidar, A. Chatterjee, M. Majee, A.L. Majumder, Synechocystis Fe superoxide dismutase gene confers oxidative stress tolerance to Escherichia coli, Biochem. Biophys. Res. Commun. 316 (2004) 540–544. https://doi.org/10.1016/j.bbrc.2004.02.084.

[61] R.V.V. Tatituri, M.B. Brenner, J. Turk, F.F. Hsu, Structural elucidation of diglycosyl diacylglycerol and monoglycosyl diacylglycerol from Streptococcus pneumoniae by multiple-stage linear ion-trap mass spectrometry with electrospray ionization, J Mass Spectrom. 47 (2012) 115–123. https://doi.org/10.1002/jms.2033.

[62] L.S. Pakkiri, B.A. Wolucka, E.J. Lubert, C.J. Waechter, Structural and topological studies on the lipid-mediated assembly of a membrane-associated

lipomannan in Micrococcus luteus, Glycobiology. 14 (2004) 73–81. https://doi.org/10.1093/glycob/cwh012.

[63] O. Montero, Lipid profiling of Synechococcus sp. PCC7002 and two related strains by HPLC coupled to ESI-(Ion Trap)-MS/MS, Z Naturforsch C Biosci. 66 (2011) 0149. https://doi.org/10.5560/znc.2011.66c0149.

[64] I.N.A. Van Bogaert, J. Zhang, W. Soetaert, Microbial synthesis of sophorolipids, Process Biochem. 46 (2011) 821–833. https://doi.org/10.1016/j.procbio.2011.01.010.

[65] R. Sturms, D. White, K.L. Vickerman, T. Hattery, S. Sundararajan, B.J. Nikolau, S. Garg, Lubricant properties of ω − 1 hydroxy branched fatty acid-containing natural and synthetic lipids, Tribol Lett. 65 (2017) 1–10. https://doi.org/10.1007/s11249-017-0883-z.

Tables and Figures

Table 1. Bacterial strains used in this study

Strain	Remarks	Source
Escherichia coli		
JM109	Competent cells	Ref. 1
Alicyclobacillus		
A. acidocalderius subsp. *acidocalderius* DSM446	Template of *aaKASIII*	Riken BioResource Center
Cupriavidus		
Cupriavidus necator H16	Template of *RphaAB*	Riken BioResource Center
Synechocystis		
wild type	Wild-type *Synechocystis* sp PCC 6803, glucose-tolerant (GT) strain	Ref. 2
KASIII+	P_{cpc}:: *aaKASIII* integrated at *fabH* in *S. 6803* genome	This study
KASIII+/phaC-	P_{cpc}:: *aaKASIII* integrated at *fabH* and deletion of *phaC* in *S. 6803* genome	This study
KASIII+/phaC-/SphaAB+	P_{cpc}:: *aaKASIII* integrated at *fabH* and P_{cpc}:: *SphaAB* at *phaC* in *S. 6803* genome	This study
KASIII+/phaC-/CphaAB+	P_{cpc}:: *aaKASIII* integrated at *fabH* and P_{cpc}:: *CphaAB* at *phaC* in *S. 6803* genome	This study

1. Yanish-Perron, C., Vieira, J. and Messing, J. (1985). **33**, 103-119. *Gene*.
2. J. G. K. Williams (1988) **167**, 766-778 *Methods Enzymol.*

Table 2. Primer sequences

No.	Primer name	Primer sequences
	Knockout for the *fabH* gene in *S.* 6803 and expression of the *aaKASIII* gene	
1	aaKASIII_F	CATATGTACAAGGCCGTGATTCG
2	aaKASIII_R	AGATCTTCAATACTCCACCATCGCGC
3	ahKASIII_F	CATATGGCGATTCGGGCAGGGAT
4	ahKASIII_R	AGATCTTTATAGCCGCAGCGCCGCGG
5	fabH_up_F	CCTGGAACAGTTTGCCCTCA
6	fabH_dn_R	TTAGGCAGGAAATAAATTGG
7	fabH_in_F	TGCGGTGGGCGATCGCCTGG
8	fabH_in_R	AAGGCAAAGGCTCTGGTGGC
9	CmCK_inf_F	CAGAGCCTTTGCCTTTCGAGCGCTGATGTCCGGCG
10	CmCK_inf_R	CGATCGCCCACCGCAAATGTGAGGTTAACAGATCT
	Knockout for the *phaC* gene and overexpression of the *phaAB* gene	
11	phaAB_up_F	CATATGGCCGCCCATCCCAA
12	phaAB_dn_R	GGATCCATTTTCCTGCTCAACAAAG
13	phaC_up_F	ATGATGGGCTCGGCTCCCCA
14	phaC_dn_R	TGCGGTGTCTGACGAGCGATTC
15	PhaC_in_F	GGAATACATTAGGGCAACAC
16	PhaC_in_R	ACTATCCATCGGATCTGAAC
17	Kam_inf_F	GATCCGATGGATAGTTTGTGTCTCAAAATCTCTGA
18	Kam_inf_R	GCCCTAATGTATTCCTCAAGTCAGCGTAATGCTCTG
19	pMD19_Km_PhaC_in_F	GGAATACATTAGGGCAACACTC
20	pMD19_Km_PhaC_in_R	TCAAGTCAGCGTAATGCTCTG
21	cpc_phaAB_inf_F	ATTACGCTGACTTGAACCTGTAGAGAAGAGTCCC
22	cpc_phaAB_inf_R	GCCCTAATGTATTCCGATCCATTTTCCTGCTCAAC
23	cpc560_R	TGAATTAATCTCCTACTTGA
24	CphaAB_inf_F	GTAGGAGATTAATTCAATGACGTTGTCATCGT
25	CphaAB_inf_R	GCCCTAATGTATTCCTCAGCCCATATGCAG
26	CphaB_in_F	CGAGCGCAAATAAGGAAG
27	nphT7_F	GTAGGAGATTAATTCAATGACCGACGTACGATTTCGA
28	nphT7_R	CTTATTTGCGCTCGCCATTCAATCAATGCGAA
29	trc_phaAB_inf_F	ATTACGCTGACTTGAGTACTGCGATGAGTGGCAGG
	Confirmation of the mutation	
30	PhaC_seg_F	TGTTCAGATCCGATGGATAG
31	PhaC_seg_R	AGATGAGTCCTGAGTGTTGC
32	CphaAB_in_seq_R	CCACACGAAAGCCATCCTTG
33	phaAB_seq_F	CCTTCATTACAGAAACGGC

Table 3. Plasmids used in this study

Plasmid	Characteristics	Source
pTCHT2031V	Carrying *slr2031up*, Cm^R, P_{trc}, *slr2031dn*, and Amp^R	Ref 2
pTC2031	Carrying *slr2031up*, Cm^R, $P_{cpc'}$ *slr2031dn*, and Amp^R	Ref 3
pEX-K4J2-nphT7	pEX with codon optimizing *nphT7*, and Km^R	eurofins genomics
pMD19_phaC	pMD19 with *phaC* from *S.* 6803, carrying Amp^R	This study
pMD19ΔphaC	pMD19 with *phaCup*, Km^R , *phaCdn*, and Amp^R	This study
pMD19ΔphaC::SphaAB	pMD19Δ*phaC*::Km^R with *phaAB* from *S.* 6803 and Amp^R	This study
pMD19ΔphaC::CphaAB	pMD19Δ*phaC*::Km^R with *phaAB* from *C. necator* H16 and Amp^R	This study
pTC_aaKASIII	Carrying *slr2031up*, Cm^R, $P_{cpc'}$, *aaKASIII*, *slr2031dn* and Amp^R	This study
pTC_SphaAB	Carrying *slr2031up*, Cm^R, $P_{cpc'}$, *SphaAB*, *slr2031dn* and Amp^R	This study
pMD19_fabH	pMD19 with *fabH* from *S.* 6803 carrying Amp^R	This study
pMD19ΔfabH::aaKASIII	pMD19 with *fabHup*, Cm^R, $P_{cpc'}$, *aaKASIII*, *fabHdn* and Amp^R	This study

3. T. Ishizuka et al. (2006) **47**, 1251-1261 *Plant Cell Physiol.*
4. S. Machida et al. (2019) **139**, 173-183 *Photosyn. Res.*

slr2031up, upstream gene of *slr2031*; *slr2031dn*, downstream gene of *slr2031*; *fabHup*, upstream gene of *fabH* for homologous recombination; *fabHdn*, downstream gene of *fabH* for homologous recombination; *phaCup*, upstream gene of *phaC* for homologous recombination; *phaCdn*, downstream gene of *phaC* for homologous recombination; Amp^R, Ampicillin resistance gene; Cm^r, chloramphenicol resistant gene; Km^r, kanamycin resistant gene; P*cpc*, cpc560 promoter.

Table 4. Fatty acid composition of each lipid class in *Synechocystis* cells

Strain	Lipid class	**Fatty acids**							
		16:0	18:0	18:1	18:2	18:3	16:0 OH	18:0 OH	18:1 OH
Wild type	MGDG	53.9 ± 3.0	1.7 ± 0.4	8.1 ± 5.3	17.6 ± 1.5	18.7 ± 0.7	-[a]	-	-
	DGDG	55.2 ± 4.4	3.9 ± 1.7	7.6 ± 1.7	21.2 ± 2.0	12.0 ± 6.0	-	-	-
	SQDG	68.9 ± 7.2	3.3 ± 1.8	11.9 ± 5.8	14.6 ± 1.0	1.3 ± 0.8	-	-	-
	PG	60.6 ± 5.7	6.9 ± 2.2	11.3 ± 2.3	24.4 ± 2.1	1.9 ± 1.2	-	-	-
	Total	48.0 ± 0.4	1.6 ± 0.2	12.3 ± 3.5	21.9 ± 2.0	16.2 ± 1.1	-	-	-
aaKASIII+/phaC-/CphaAB+	MGDG	50.3 ± 3.9	2.6 ± 1.0	12.1 ± 6.0	19.6 ± 1.4	15.5 ± 1.3	t[b]*	t*	t*
	DGDG	50.4 ± 1.5	4.6 ± 2.1	9.1 ± 1.8	20.9 ± 2.9	14.9 ± 0.9	0.1 ± 0.0*	-	t*
	SQDG	56.0 ± 1.5	5.4 ± 0.8	18.6 ± 4.5	18.6 ± 2.7	0.6 ± 0.1	0.5 ± 0.2	t	0.3 ± 0.1
	PG	51.1 ± 1.4	7.3 ± 3.8	15.2 ± 2.5	24.1± 1.7	1.5 ± 0.2	0.4 ± 0.1	t	0.5 ± 0.2
	Total	45.1 ± 0.8	3.3 ± 0.4	15.6 ± 4.3	22.2 ± 3.0	12.6 ± 1.6	0.6 ± 0.1	0.1 ± 0.0	0.7 ± 0.2

[a]Not detected

[b]Trace amount (less than 0.04%)

*Significant difference was indicated by Student's *t*-test when compared with total lipid ($P < 0.05$)

Table 5. Bond cleavage of the molecules on positive ion mode and estimation of fatty acid species.

Peak	Retention time	*m/z*							Estimation	
No.	(min)	$[M+K]^+$	$[M+Na]^+$	**a**	**b**	**c**	**d**	**e**	Head group	Fatty acids
1	19.25	807.50	791.52	589.48	571.47	335.26	311.26	261.22	$C_6H_{12}O_6$	16:0 OH, 18:3
2	20.07	809.51	793.54	591.49	573.48	337.27	311.26	263.24	$C_6H_{12}O_6$	16:0 OH, 18:2
3	21.06	811.53	795.56	593.51	575.50	339.29	311.26	265.25	$C_6H_{12}O_6$	16:0 OH, 18:1
4	21.57	811.53	795.56	595.51	575.50	337.27	313.27	263.24	$C_6H_{12}O_6$	16:0, 18:1 OH
5	22.23	813.54	797.57	595.53	577.52	341.30	311.26	254.42	$C_6H_{12}O_6$	16:0 OH, 18:0

Table 6. Major molecular species on negative ion mode and exact calculated mass from the estimation from positive ion mode**.**

Peak No.	Retention time	Calculated	*m/z*	
	(min)	exact mass	$[M+HCOO]^-$	$[M-H]^-$
1	N.D.[a]	768.54	N.D.	N.D.
2	19.78	770.55	815.55	769.54
3	20.77	772.57	817.57	771.56
4	21.29	772.57	817.57	771.56
5	N.D.	774.59	N.D.	N.D.

[a]Not detected

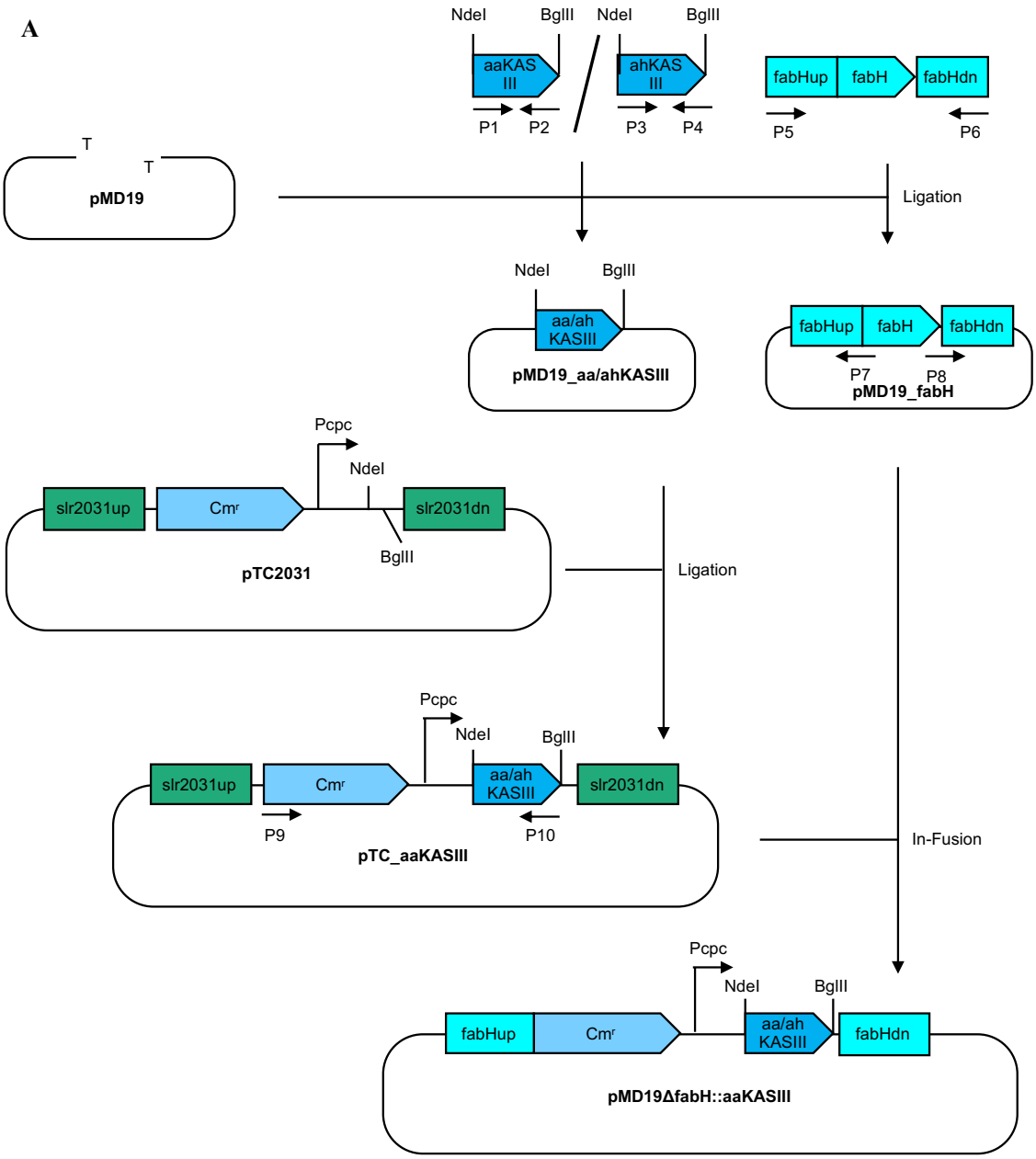
A
NdeI
BglII
NdeI
BglII
aaKAS III
ahKAS III
P1
P2
P3
P4
fabHup
fabH
fabHdn
P5
P6
T
T
pMD19
Ligation
NdeI
BglII
aa/ah KASIII
pMD19_aa/ahKASIII
fabHup
fabH
fabHdn
P7
P8
pMD19_fabH
Pcpc
NdeI
slr2031up
Cmr
slr2031dn
BglII
pTC2031
Ligation
Pcpc
NdeI
BglII
slr2031up
Cmr
aa/ah KASIII
slr2031dn
P9
P10
pTC_aaKASIII
In-Fusion
Pcpc
NdeI
BglII
fabHup
Cmr
aa/ah KASIII
fabHdn
pMD19ΔfabH::aaKASIII

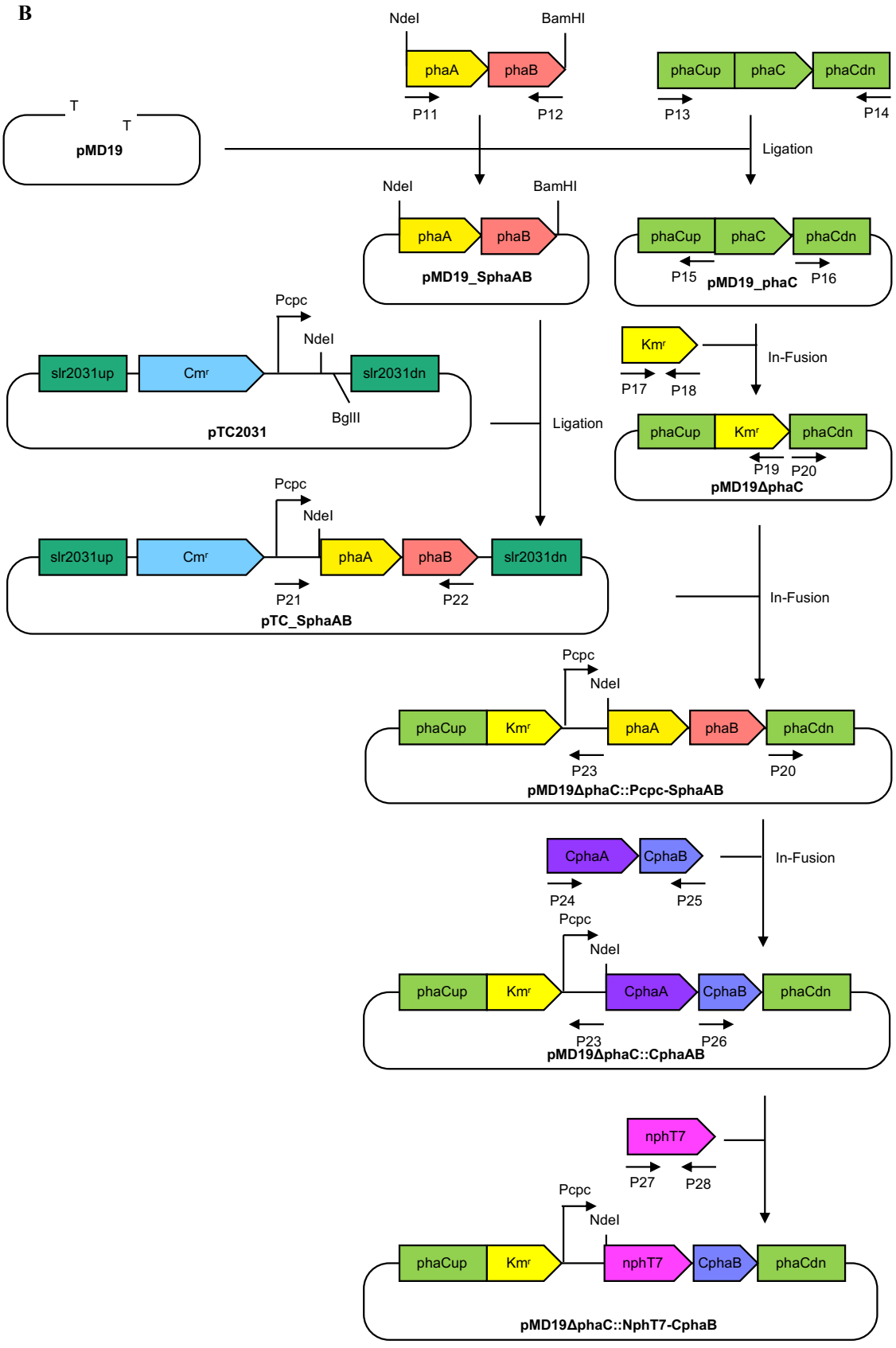
B
NdeI
BamHI
phaA
phaB
P11
P12
phaCup
phaC
phaCdn
P13
P14
T
T
pMD19
Ligation
NdeI
BamHI
phaA
phaB
pMD19_SphaAB
phaCup
phaC
phaCdn
P15
pMD19_phaC
P16
Pcpc
NdeI
slr2031up
Cmr
slr2031dn
BglII
pTC2031
Kmr
P17
P18
In-Fusion
Ligation
phaCup
Kmr
phaCdn
P19
P20
pMD19ΔphaC
Pcpc
NdeI
slr2031up
Cmr
phaA
phaB
slr2031dn
P21
P22
pTC_SphaAB
In-Fusion
Pcpc
NdeI
phaCup
Kmr
phaA
phaB
phaCdn
P23
P20
pMD19ΔphaC::Pcpc-SphaAB
CphaA
CphaB
P24
P25
In-Fusion
Pcpc
NdeI
phaCup
Kmr
CphaA
CphaB
phaCdn
P23
P26
pMD19ΔphaC::CphaAB
nphT7
P27
P28
Pcpc
NdeI
phaCup
Kmr
nphT7
CphaB
phaCdn
pMD19ΔphaC::NphT7-CphaB

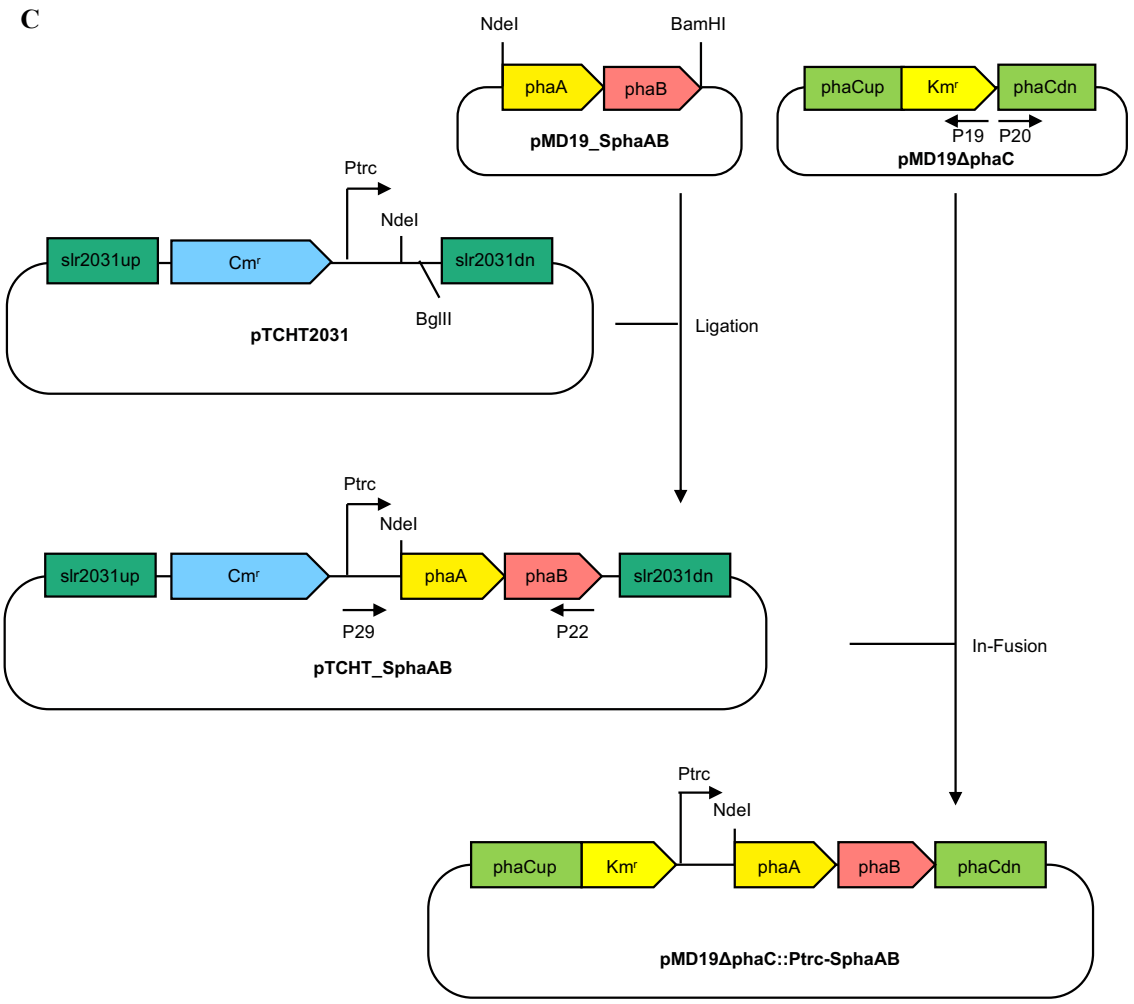

Figure 1. Construction of the plasmids.

(A) Schematic overview of the engineering of the DNA fragments for simultaneous deletion of native *fabH* and expression of *aaKASIII* in *Synechocystis* cells, (B) For deletion of *phaC* and expression of *phaAB*, C*phaAB* or *nphT7-CphaB* expressed by *cpc560* promoter. (C) For deletion of *phaC* and expression of *phaAB* expressed by *trc* promoter. The fragments encoding aaKASIII were amplified from *Alicyclobacillus acidocalderius and CphaAB* were amplified from *Cupriavidus necator.* slr2031up, upstream gene of *slr2031*; slr2031dn, downstream gene of *slr2031*; fabHup, upstream gene of *fabH* for homologous recombination; fabHdn, downstream gene of *fabH* for homologous recombination; phaCup, upstream gene of *phaC* for homologous recombination; phaCdn, downstream gene of *phaC* for homologous recombination; Cm^r, chloramphenicol resistant gene; Km^r, kanamycin resistant gene; Pcpc, cpc560 promoter; Ptrc, trc promoter.

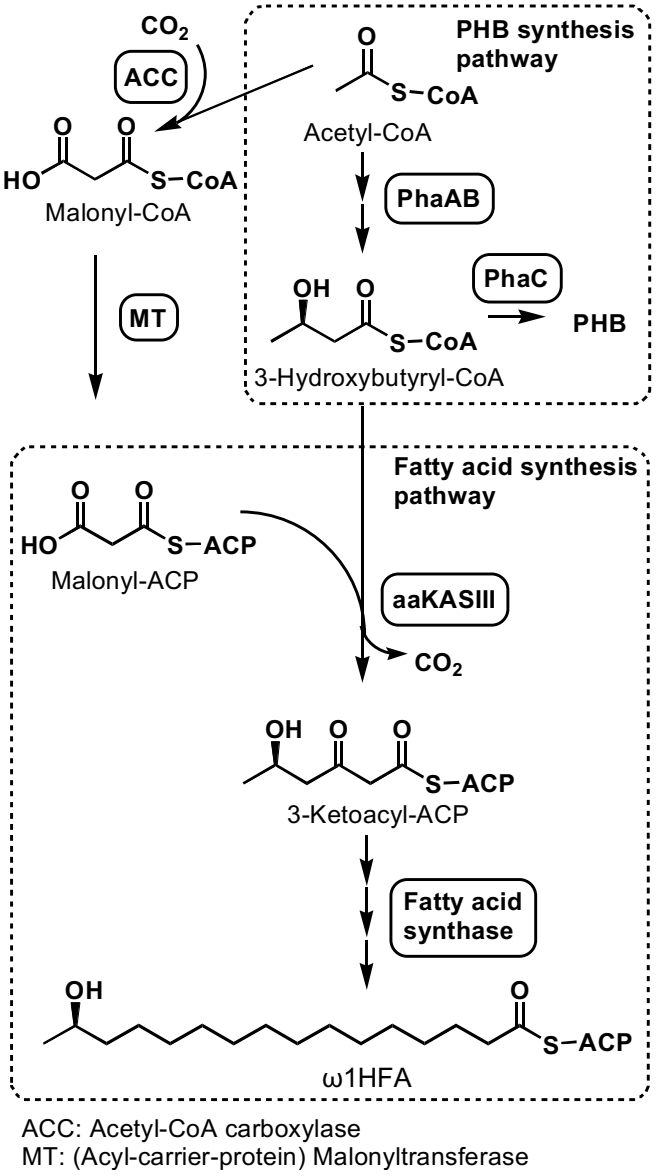

Figure 2. Pathway for production of the ω1HFA.

3HB-CoA is synthesized from acetyl-CoA via two step reaction of the enzymes, PhaA and PhaB. PHB is synthesized from 3HB-CoA by PhaC and PhaE. ω1HFAs were synthesized from 3HB-CoA introduced into the FA synthetic pathway by catalyzing aaKASIII in a *Synechocystis* deleted the PhaC activity. ACC, MT, PHB, and ACP indicate acetyl-CoA carboxylase, malonyl coenzyme A-acyl carrier protein transacylase, polyhydroxybutyrate, and acyl carrier protein, respectively.

```
  1  M  T  D  V  R  F  R  I  I  G  T  G  A  Y  V  P  E  R  I  V  20
  1 ATGACCGACGTaCGATTtCGaATTATtGGcACaGGcGCtTACGTcCCGGAgCGcATtGTg 60

 21  S  N  D  E  V  G  A  P  A  G  V  D  D  D  W  I  T  R  K  T  40
 61 agtAAtGAcGAgGTCGGgGCaCCGGCgGGcGTGGAtGAtGACTGGATtACaCGgAAaACC 120

 41  G  I  R  Q  R  R  W  A  A  D  D  Q  A  T  S  D  L  A  T  A  60
121 GGcATCCGGCAaCGTCGtTGGGCtGCaGAtGACCAaGCaACaTCtGAttTaGCtACtGCt 180

 61  A  G  R  A  A  L  K  A  A  G  I  T  P  E  Q  L  T  V  I  A  80
181 GCtGGaCGcGCcGCaCTGAAgGCtGCGGGgATCACGCCCGAaCAGCTcACaGTcATCGCa 240

 81  V  A  T  S  T  P  D  R  P  Q  P  P  T  A  A  Y  V  Q  H  H  100
241 GTaGCtACCagtACcCCGGACCGtCCcCAGCCGCCtACGGCaGCgTATGTtCAGCAtCAt 300

101  L  G  A  T  G  T  A  A  F  D  V  N  A  V  C  S  G  T  V  F  120
301 CTaGGcGCGACtGGtACTGCcGCaTTCGAtGTtAACGCtGTtTGtTCtGGaACCGTGTTt 360

121  A  L  S  S  V  A  G  T  L  V  Y  R  G  G  Y  A  L  V  I  G  140
361 GCatTaagtTCtGTcGCGGGaACCCTgGTcTAtCGaGGgGGaTAtGCGCTaGTaATCGGa 420

141  A  D  L  Y  S  R  I  L  N  P  A  D  R  K  T  V  V  L  F  G  160
421 GCaGACCTcTACagcCGCATCtTaAAtCCaGCgGAtCGaAAGACtGTCGTaCTcTTCGGa 480

161  D  G  A  G  A  M  V  L  G  P  T  S  T  G  T  G  P  I  V  R  180
481 GAtGGaGCtGGCGCcATGGTaCTCGGcCCaACCTCtACCGGCACtGGCCCaATCGTtCGc 540

181  R  V  A  L  H  T  F  G  G  L  T  D  L  I  R  V  P  A  G  G  200
541 CGtGTCGCgCTaCAtACgTTtGGgGGtCTCACaGAttTGATCCGTGTaCCtGCGGGgGGt 600

201  S  R  Q  P  L  D  T  D  G  L  D  A  G  L  Q  Y  F  A  M  D  220
601 AGtCGCCAaCCaCTGGACACtGAcGGgtTaGACGCcGGtCTGCAaTACTTtGCtATGGAt 660

221  G  R  E  V  R  R  F  V  T  E  H  L  P  Q  L  I  K  G  F  L  240
661 GGcCGcGAaGTcCGaCGaTTCGTgACGGAaCACtTGCCGCAaCTaATtAAGGGaTTtCTG 720

241  H  E  A  G  V  D  A  A  D  I  S  H  F  V  P  H  Q  A  N  G  260
721 CAtGAaGCCGGcGTCGACGCaGCgGACATCAGCCAtTTCGTtCCcCATCAaGCtAACGGg 780

261  V  M  L  D  E  V  F  G  E  L  H  L  P  R  A  T  M  H  R  T  280
781 GTCATGtTgGAtGAGGTaTTtGGtGAatTGCATtTGCCGCGcGCcACaATGCACCGaACc 840

281  V  E  T  Y  G  N  T  G  A  A  S  I  P  I  T  M  D  A  A  V  300
841 GTaGAaACtTACGGgAAtACtGGgGCaGCaTCCATtCCcATCACaATGGAtGCaGCgGTa 900

301  R  A  G  S  F  R  P  G  E  L  V  L  L  A  G  F  G  G  G  M  320
901 CGCGCgGGcagCTTCCGtCCtGGCGAatTaGTatTaCTGGCaGGaTTtGGgGGCGGtATG 960

321  A  A  S  F  A  L  I  E  W  329
961 GCtGCaAGtTTCGCatTGATtGAaTGG 987
```

Figure 3. The sequence of codon-optimized *nphT7*.

Upper sequence is amino acid sequence and lower one is nucleotide sequence of codon optimized *nphT7*. Small letter is the replaced nucleotide.

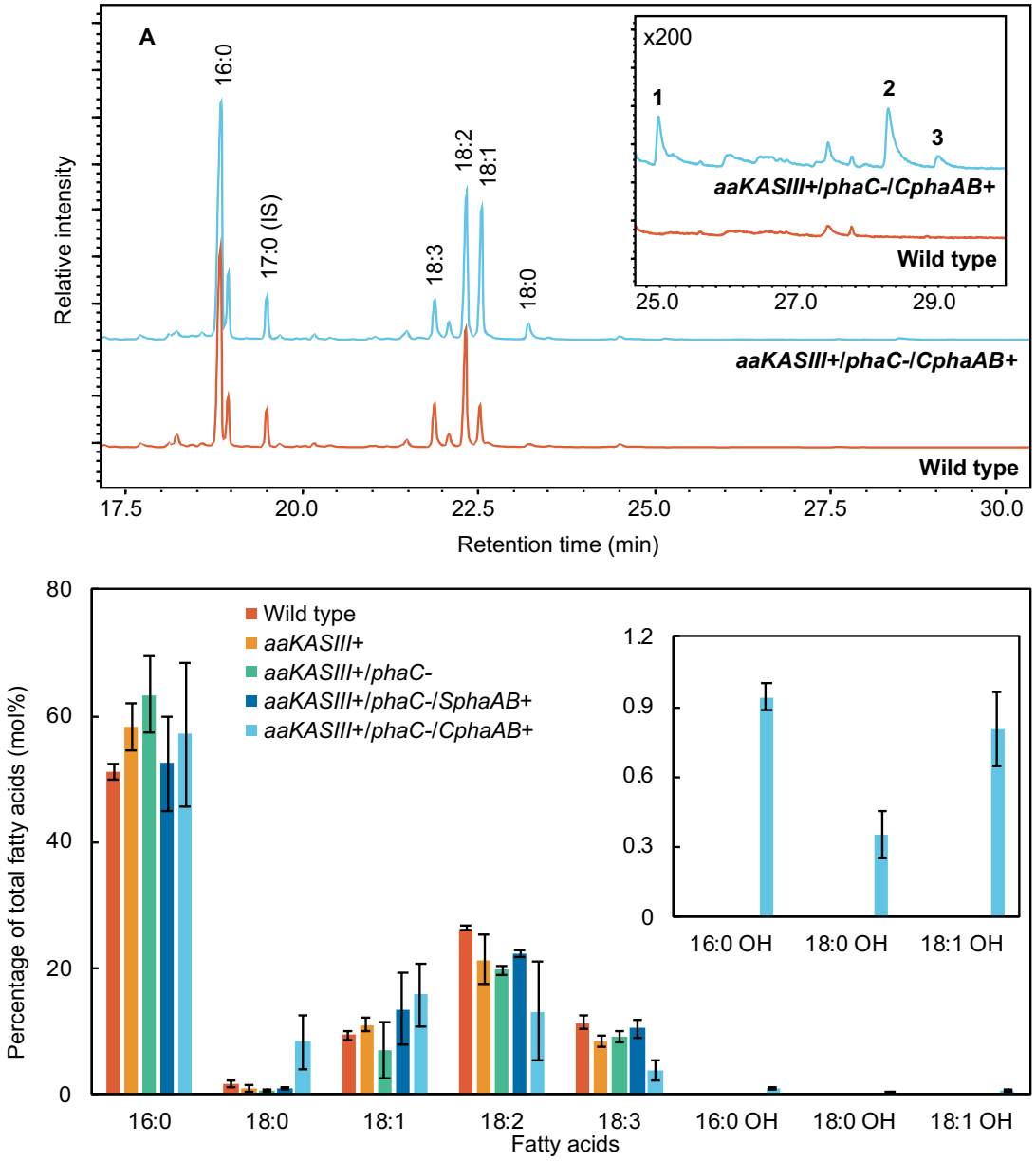

Figure 4. ω1HFA production in *Synechocystis*.

(A) Gas chromatogram of FAME from the lipids extracted from the *aaKASIII+/phaC-/CphaAB+* and wild-type cells. (B) The production of the ω1HFAs in wild-type and the genetically engineered cells of *Synechocystis*. 16:0, 18:0, 18:1, 18:2, 18:3, 16:0 OH. 18:0 OH, and 18:1 OH indicate palmitic acid, stearic acid, oleic acid, linoleic acid, γ-linolenic acid, 15-hydroxyhexadecanoic acid, 17-hydroxyoctadecanoic acid, and 17-hydroxyoctadec-9-enoic acid, respectively. Each data point is an average of 3 independent experiments and the error bars indicate the standard deviations.

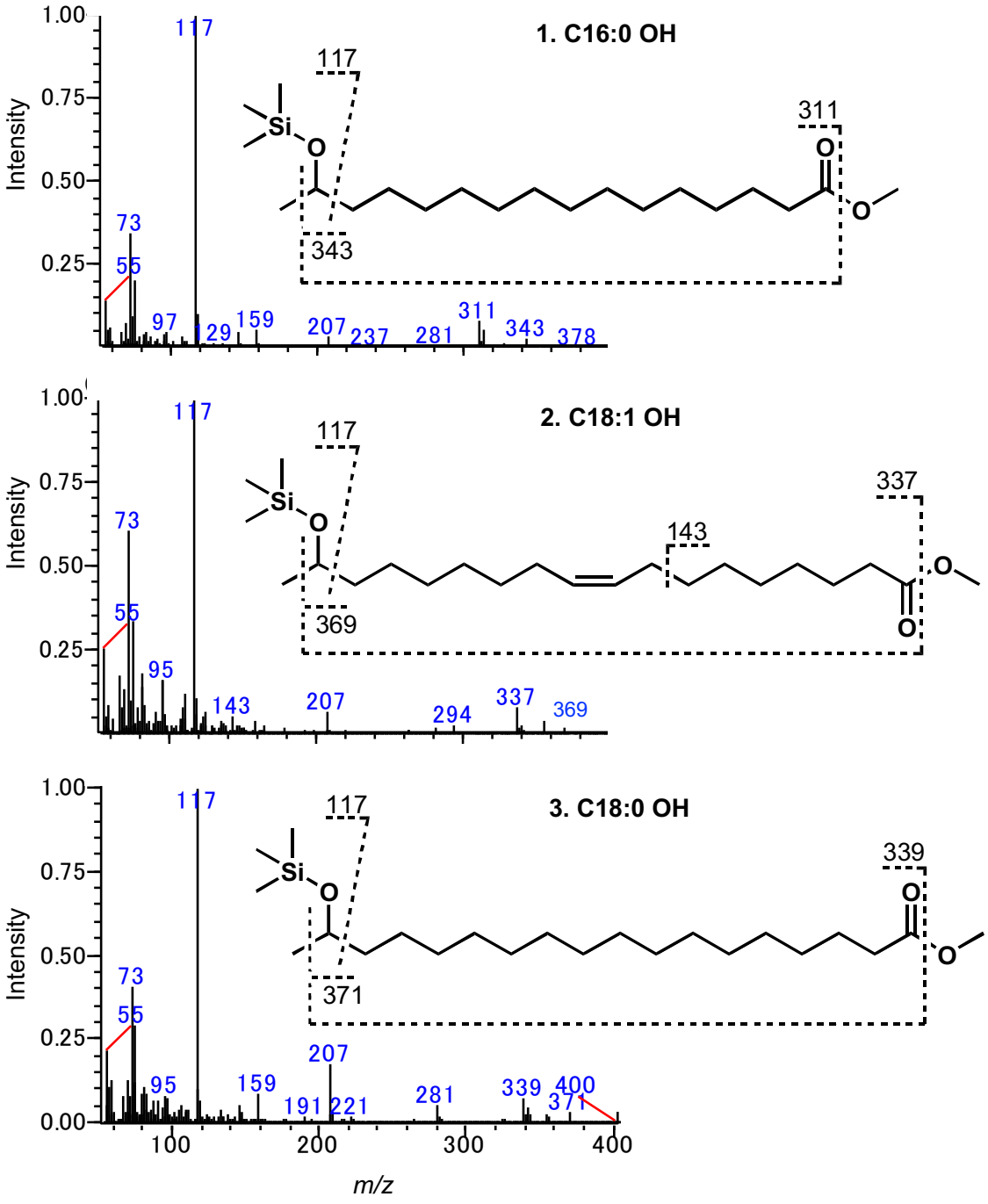

Figure 5. Mass-spectra confirmation of ω1HFAs

Mass-spectra confirmation of peak 1, 2 and 3 on Fig 2A. Consistent with the analytical chemistry used to prepare these samples, these peaks are identified as the silylated-form of the methyl-ester of ω1HFAs, and this metabolite is absent from wild-type. 1. 15-hydroxy hexadecanoic acid; 2. 17-hydroxy octadic-9-enoic acid; 3. 17-hydroxy octadecanoic acid

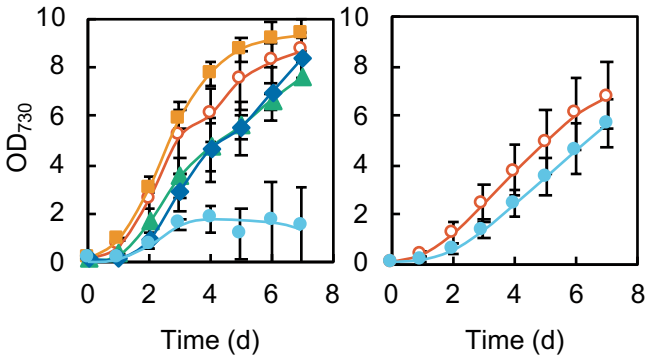

Figure 6. Growth of the wild-type and recombinant cells of *Synechocystis*.
(A) Growths of the wild-type, *aaKASIII+*, *aaKASIII+/phaC-*, *aaKASIII+/phaC-/SphaAB+*, and *aaKASIII+/phaC-/CphaAB+* cultivated under 70 µmol m^{-2} s^{-1}were indicated by open circles, squares, triangles, diamonds, and closed circles, respectively. (B) Growths of the wild type and *aaKASIII+/phaC-/CphaAB+* cultivated under 35 µmol m^{-2} s^{-1} were indicated by open and closed circles, respectively.

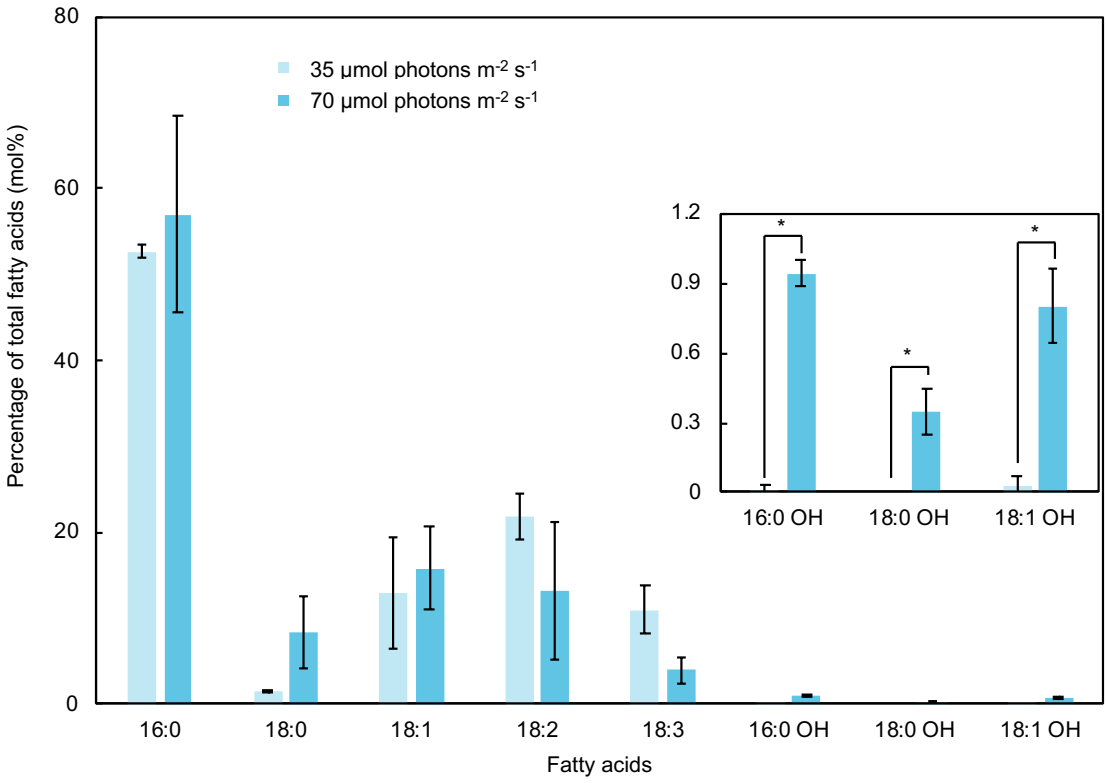

Figure 7. Production of the ω1HFAs in the *aaKASIII*+/*phaC*-/*CphaAB*+ under 35 µmol photons m^{-2} s^{-1} and 70 µmol photons m^{-2} s^{-1}.

Each data point is an average of 3 independent experiments and the error bars indicate the standard deviations. Asterisks indicate significant differences (*$P < 0.01$, Student's *t*-test).

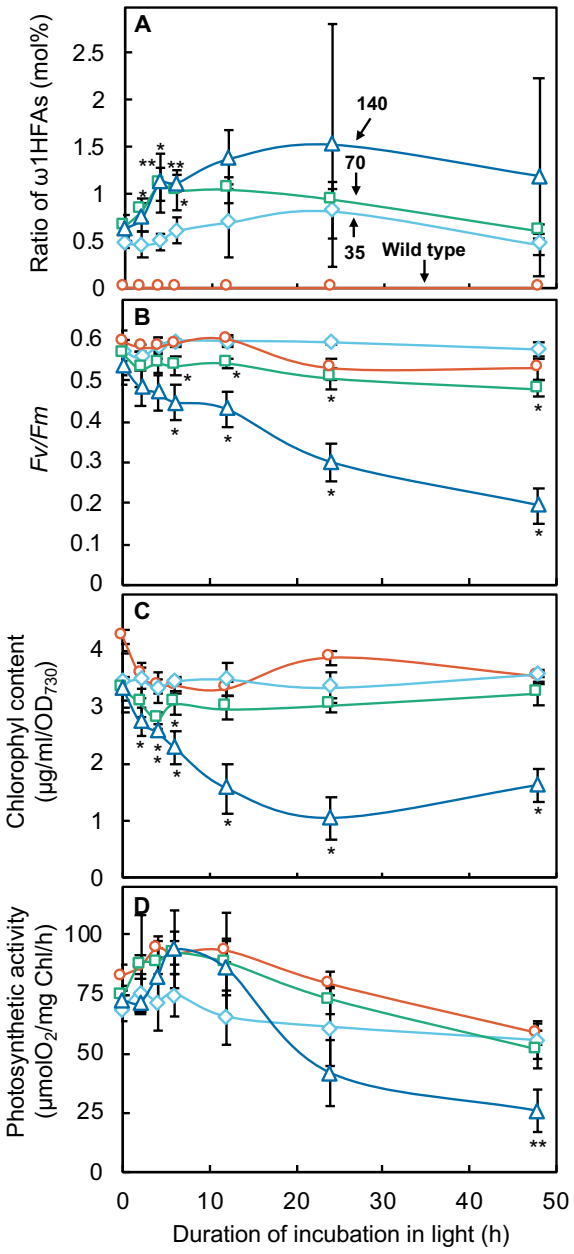

Figure 8. Effects of the light intensity on ω1HFAs production and photosynthetic parameter.

(A) Production of the ω1HFAs, (B) Photosynthetic yield, (C) Chlorophyll content, and (D) Photosynthetic O_2-evolving activity of the *aaKASIII+/phaC-/CphaAB+* mutant grown under 35 μmol photons m^{-2} s^{-1} (diamonds), 70 μmol photons m^{-2} s^{-1} (squares), 140 μmol photons m^{-2} s^{-1} (triangles) and wild-type grown under 140 μmol photons m^{-2} s^{-1} (circles). Asterisks indicate significant differences compared with the *aaKASIII+/phaC-/CphaAB+* cells under 35 μmol photons m^{-2} s^{-1} (*$P < 0.05$, **$P < 0.02$, Student's *t*-test).

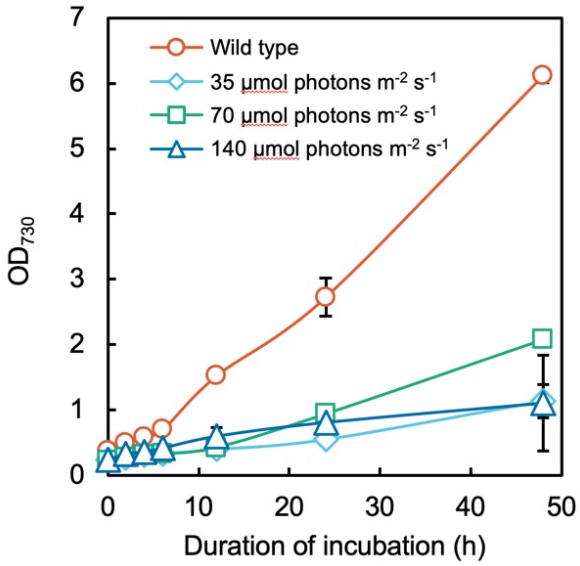

Figure 9. Effects of the light intensity on growth of the *aaKASIII+/phaC-/CphaAB+*. The transformant grown under 35 µmol photons m^{-2} s^{-1} (diamonds), 70 µmol photons m^{-2} s^{-1} (squares), 140 µmol photons m^{-2} s^{-1} (triangles) and the wild-type cells grown under 140 µmol photons m^{-2} s^{-1} (open circles)

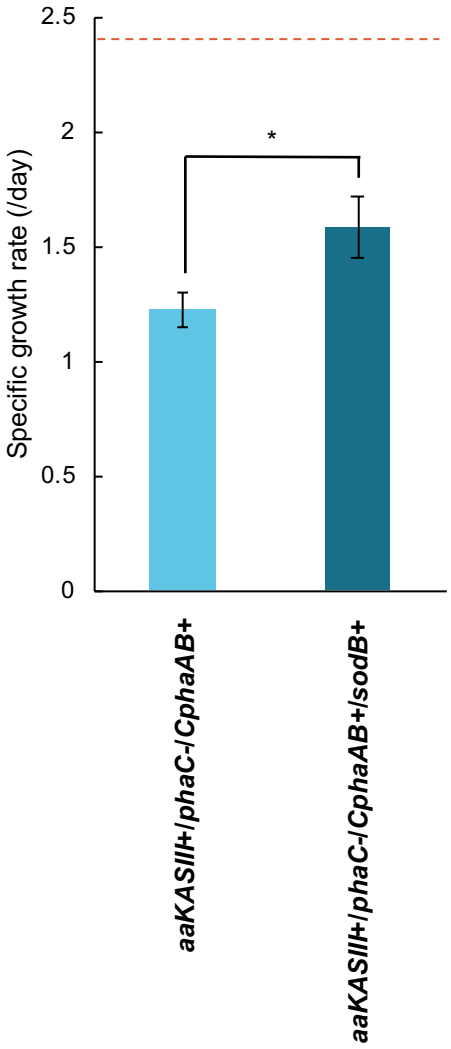

Figure 10. Comparison between specific growth rate of *aaKASIII+/phaC-/CphaAB+* and *aaKASIII+/phaC-/CphaAB+/sodB+* under 140 µmol photons m^{-2} s^{-1}. The red dashed line indicates the growth rate of the wild type cells. Each data point represents an average of 5 independent experiments, and the error bars indicate the standard deviations. Asterisks indicate significant differences (*$P < 0.05$, Student's *t*-test).

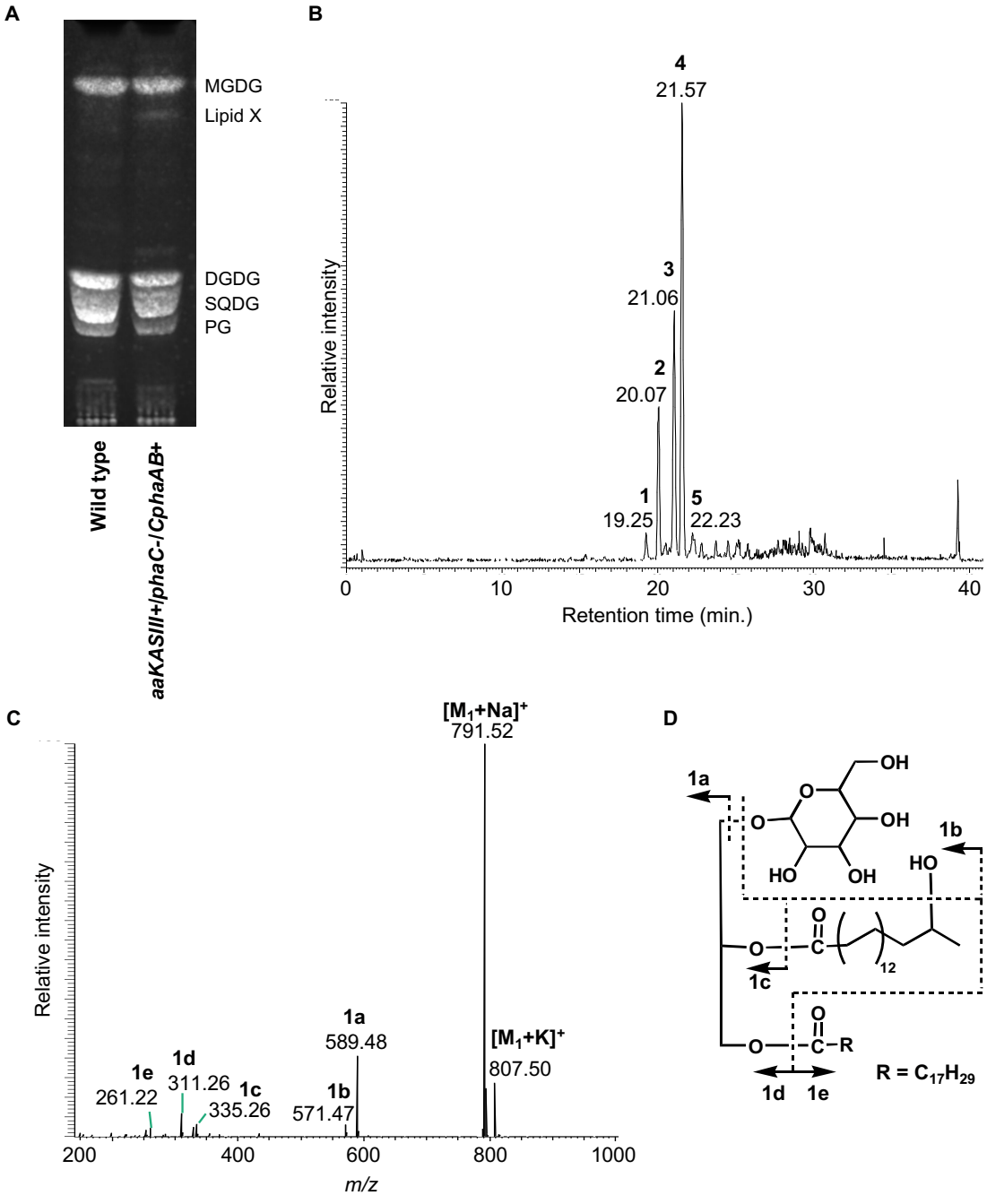

Figure 11. Analysis of novel spot on Thin-layer chromatography.

(A) Thin-layer chromatography (TLC) analysis of lipid extracts from wild-type and *aaKASIII+/phaC-/CphaAB+* lines. (B) Base peak chromatograms obtained in the LC-MS analysis of lipid X with positive ionization. (C) Mass spectra of peak **1** in positive ion mode. (D) The proposed molecular structure and fragmentation of peak **1**.

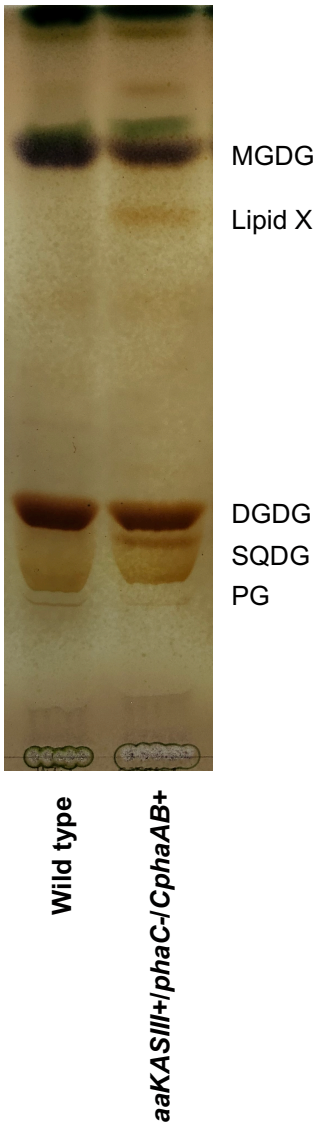

Figure 12. Visualization of lipids on the TLC plate by α-naphthol.

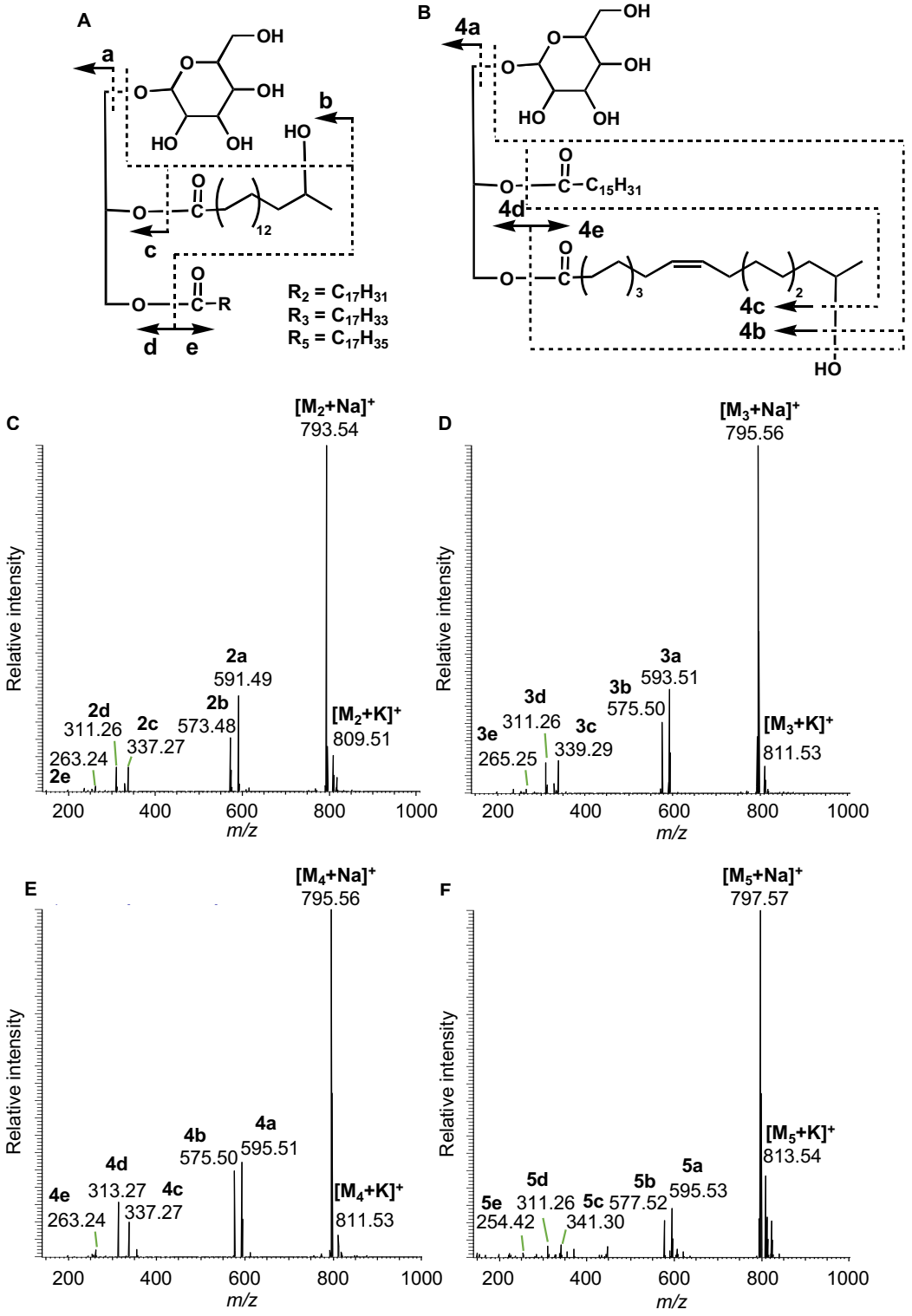

Figure 13. Proposed molecular structure and fragmentation in positive ion mode. (A) Fragmentation of peak **2**, **3** and **5,** and (B) of peak **4.** Mass spectra (C) of peak 2, (D) of peak 3, (E) of peak **4**, (F) and peak **5** in positive ion mode.

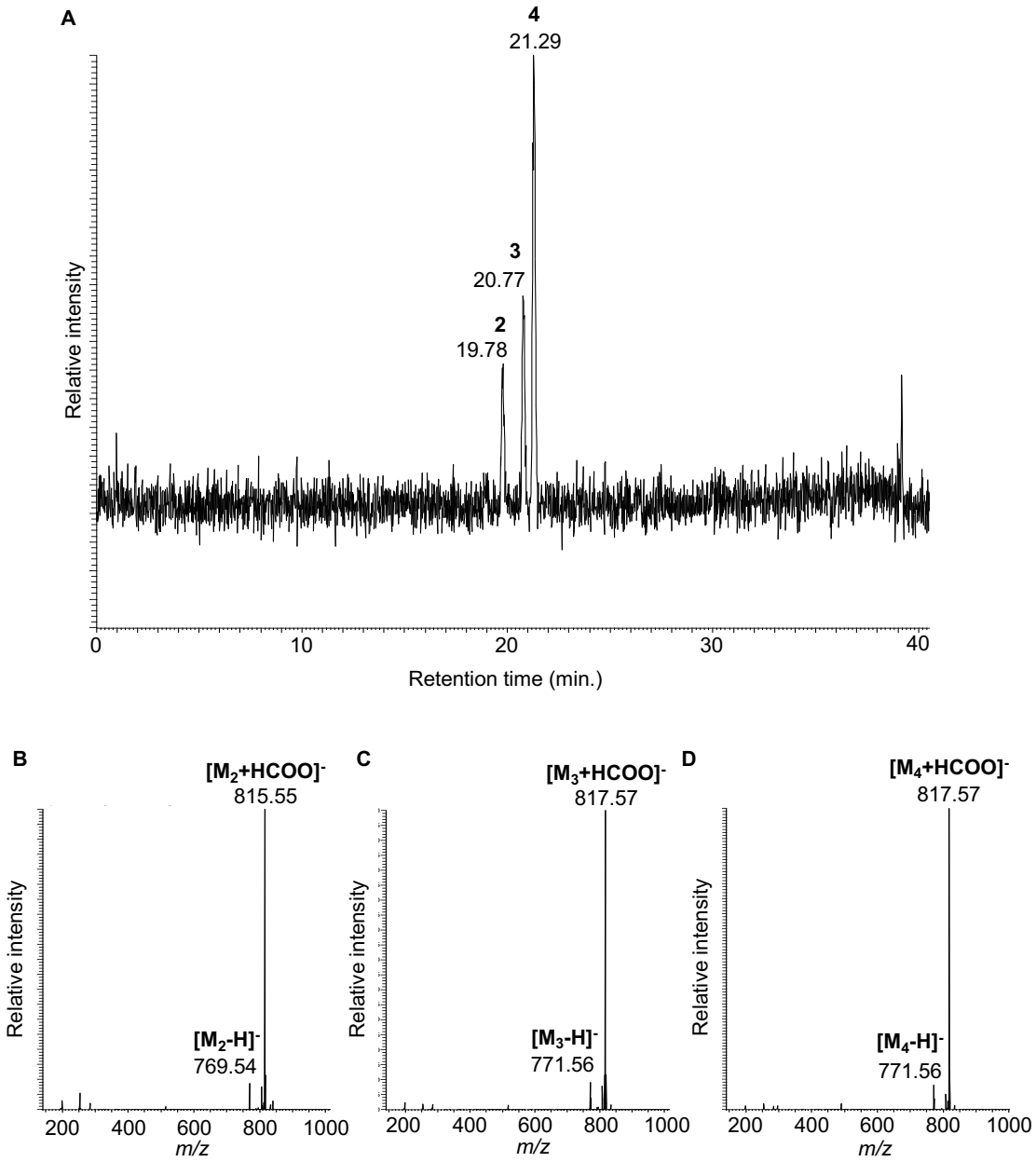

Figure 14. LC-MS analysis of lipid X with negative ionization

(A) Base peak chromatograms. Mass spectra of (B) peak 2, (C) peak 3 and (D) peak 4.